CHAPTER 3

Architecture considerations for G-N like network based on ENU's

Chapter Introduction

Almost the entire corpus of current literature on pulse-coded neural networks (PCNN) uses arguments and analyses based on the presumption of steady-state tetanus inputs in which activity level is coded by firing rate. This has a tendency to promote a presumption that PCNN analogs to non-pulsing networks based on level-coding can be obtained by a simple mapping and scaling process of some sort. This assumption can be traced all the way back to Von Neumann [von Neumann 1958].

As this chapter demonstrates, this presupposition is wholly unwarranted. The actual "in vivo" environment of PCNN systems produces a much more diverse set of firing patterns. The function of the network is strongly affected by surprisingly small variations in the firing pattern. This makes functional mapping from traditional neural network systems to PCNN systems much more challenging than has been presumed. The findings reported in this chapter reveal that PCNN functional architecture is a new topic within neural network theory for which there is much yet to be learned.

This chapter presents the detailed step-by-step process through which the final Eckhorn dipole network was achieved. The methodology employed here was first established by Grossberg in 1978 for level-coded neural networks [Grossberg 1978]. Perhaps the most significant lesson learned from this study is: the non-linear effects in PCNN signaling belong to a class of non-linear system theory so unlike older neural network analysis that functional design of PCNN systems should be approached in a two-

step process. First, the functional capabilities should be developed at the G-N network level. Second, the functioning G-N should be mapped to a functionally equivalent PCNN. This chapter illustrates how this was accomplished for dipole network using Grossberg's methodology.

The Direct Network

Before outputs from Grossberg's network (G-N) can be used for performance reference a working Eckhorn dipole network (E-DN) is required. The first goal in the design process will therefore be to achieve an E-DN whose network properties resemble G-DN (Grossberg dipole network). This means G-DN will be the functional model for designing the E-DN.

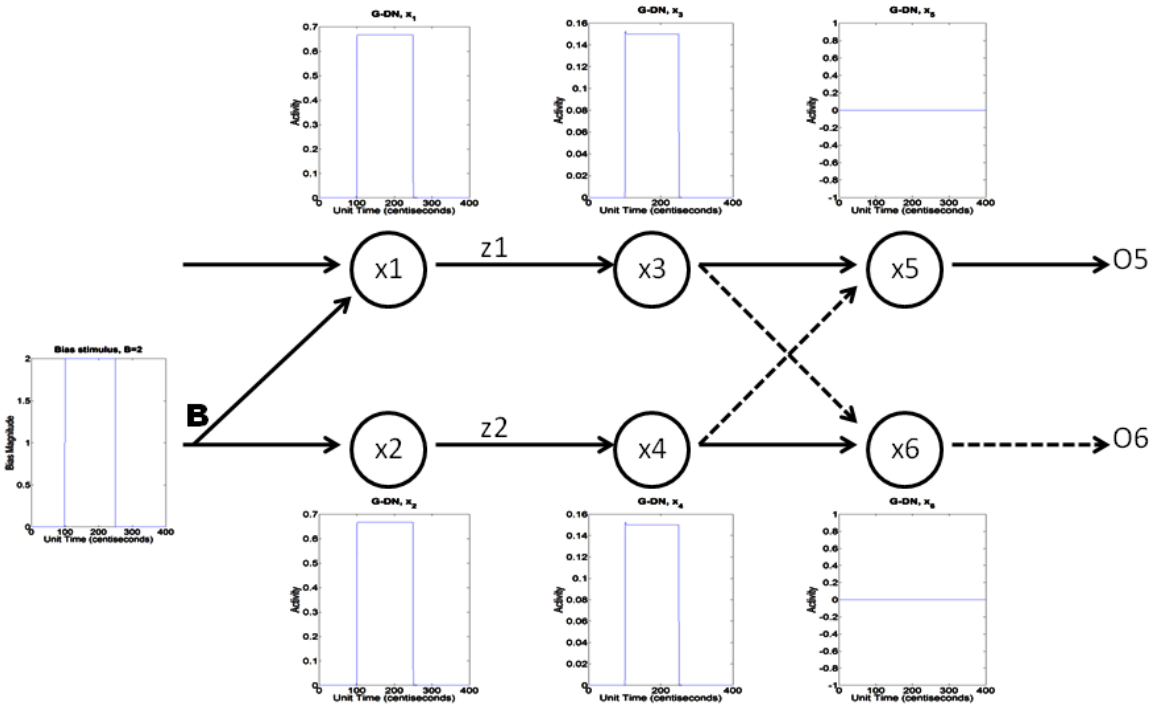

Figure 3.1. G-DN (Grossberg's Dipole Network) receiving just bias (B) stimulus.

We start with G-DN (Fig. 2.2) but with the simplest input-output relationship, i.e., with only bias input (B-input), as shown in Figure 3.1. The initial nodes (x1 & x2) receiving the same stimulus causes excitation of the succeeding nodes, x3 and x4 respectively with equal strength. This leads to cancellation of equal input strengths during cross-inhibition resulting in no activities at x5 and x6 nodes (Fig. 3.2).

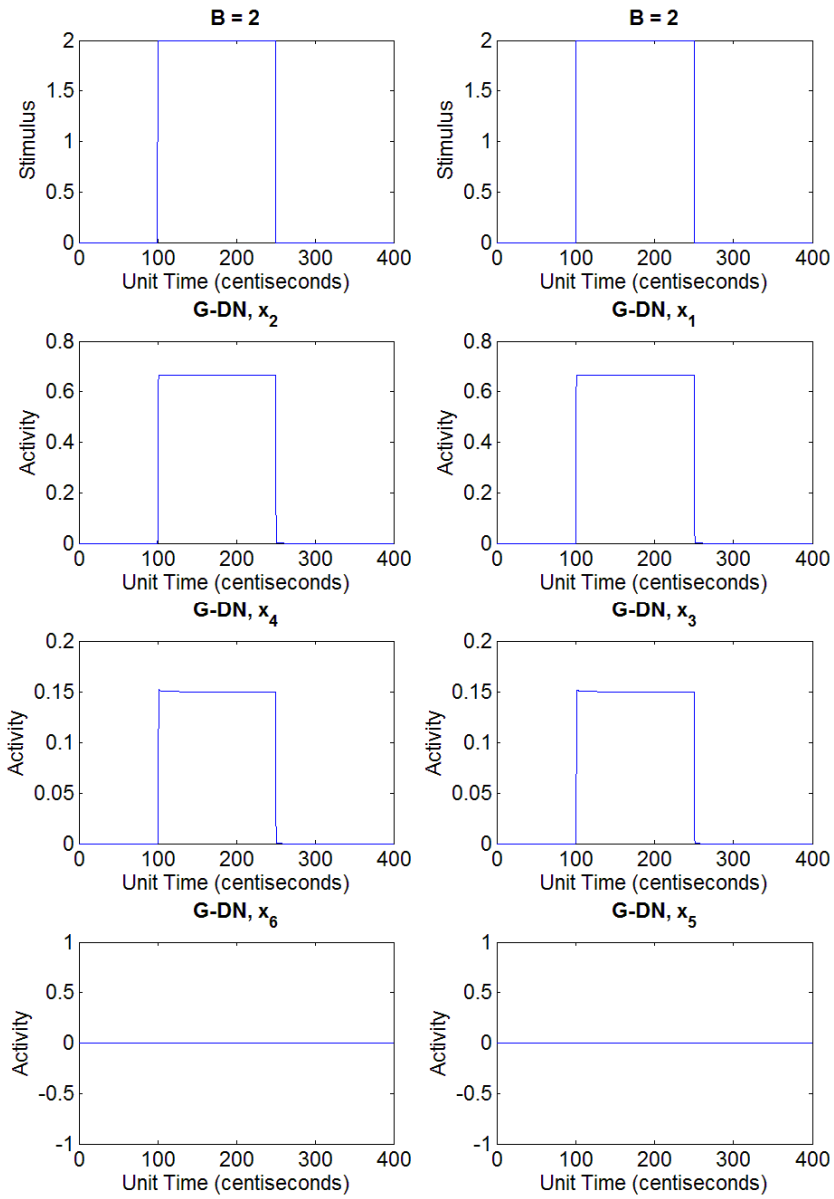

Figure 3.2. Output traces of G-DN in Figure 3.1 (inset) with just B-stimulus showing no activities in x5 & x6 nodes due to cancellation of incoming activities from x3 & x4 of equal strength.

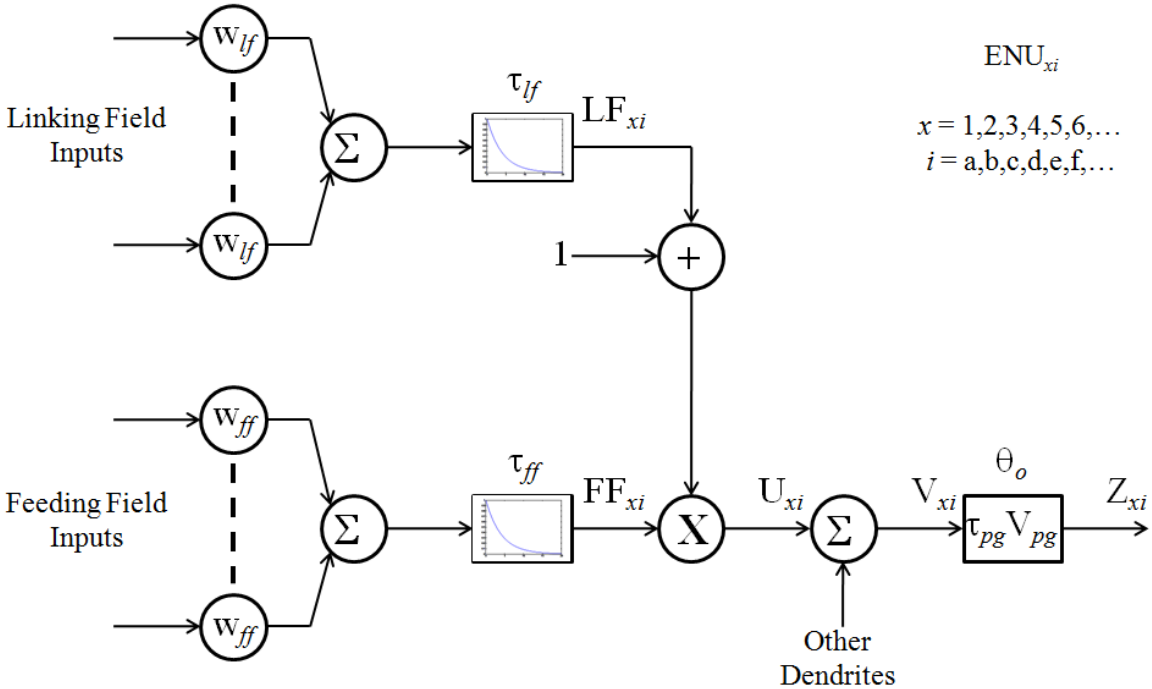

Figure 3.3. Another view of the ENU architecture showing the basic ENU (as seen in Fig. 2.11). Subscript of ENU$_{xi}$ is such that i denote one of the basic ENU shown above while x denotes the ENU group composed of the basic ENU's. The feeding field input value is either 0 or 1.
Linking field: w_{lf} & τ_{lf} are parameters (weight & time constant) and LF_{xi} the output.
Feeding field: w_{ff} & τ_{lf} are parameters (weight & time constant) and FF_{xi} the output.
Soma/Neuromime Pulse Generator (NMPG): τ_{pg}, V_{pg} & θ_o (time constant, voltage amplitude & threshold offset) and Z_{xi} spike output.

The ENU with basic configuration as shown in Figure 3.3 and with set parameters is required for constructing an E-DN analogue that would have the property as shown in Figure 3.1. The inhibitory input of a basic ENU includes an inhibitory dendrite with just the feeding field (without linking field) whose output is connected to the soma/NMPG by summation with other dendrites outputs. It should also be noted that the basic ENU implemented in the E-DN has a uniform weight value (either w_{lf} or w_{ff}) within the linking field or feeding field of the respective ENU$_x$ group. A node within E-DN may comprise more than one ENU$_x$ group.

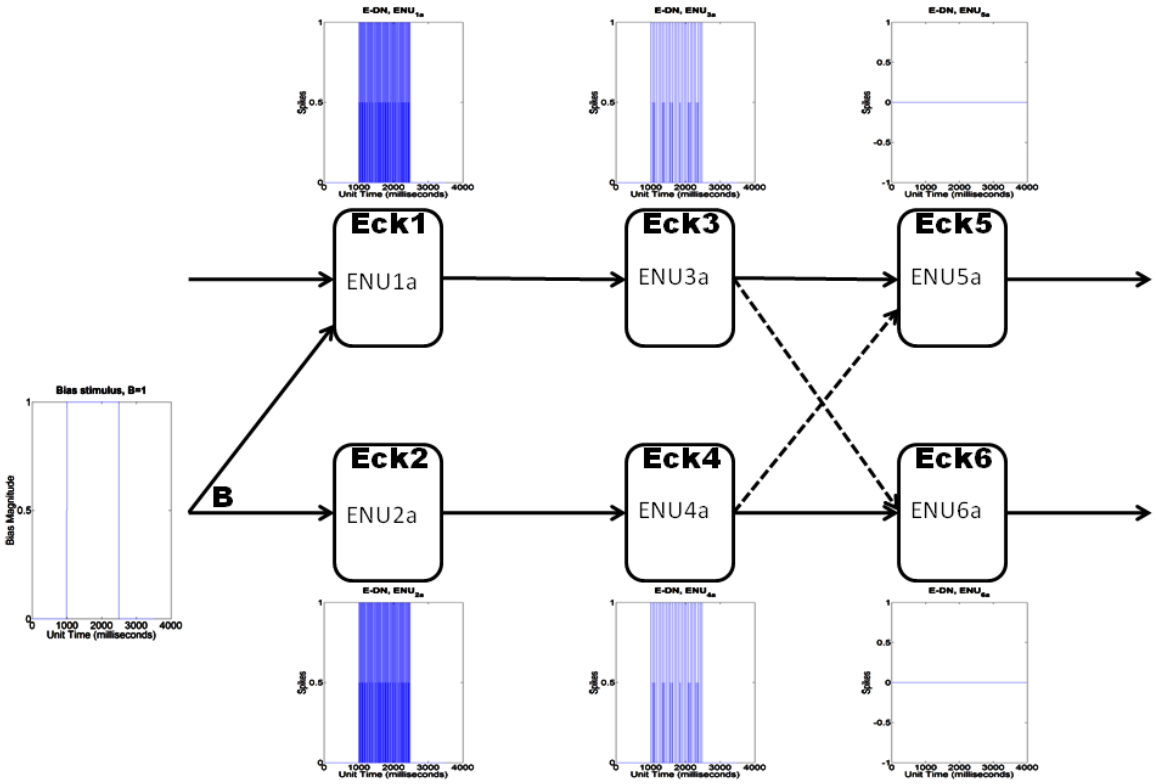

Figure 3.4. E-DN receiving just bias (B) stimulus as an Eckhorn analogue of Figure 3.1. Each node (Eck1 to Eck6) is made up of a single ENU. The figure shows outputs from respective ENU's following simulation with B-stimulus (as DC/constant) during a particular interval (1 to 2.5 seconds). A larger view of these outputs is shown in Figure 3.5. The parameter values of the simulation are shown in table 3.1.

To achieve an Eckhorn analogue of G-DN shown in Figure 3.1, the E-DN constructed (Fig. 3.4) is composed of six nodes each containing 1 ENU group and each group formed by a single basic ENU. Simulation with just B-input results in similar outcome as seen with G-DN where ENU in the node-5 (Eck5) and node-6 (Eck6) do not produce any spikes (outputs in Fig. 3.4 or Fig. 3.5 for larger view). Note that though the neuronal population are PCN's (pulse-coded neurons), to achieve an initial working model of E-DN DC (constant) input stimulus was chosen for simplicity. However, later all bias and drive inputs will be implemented as pulse trains.

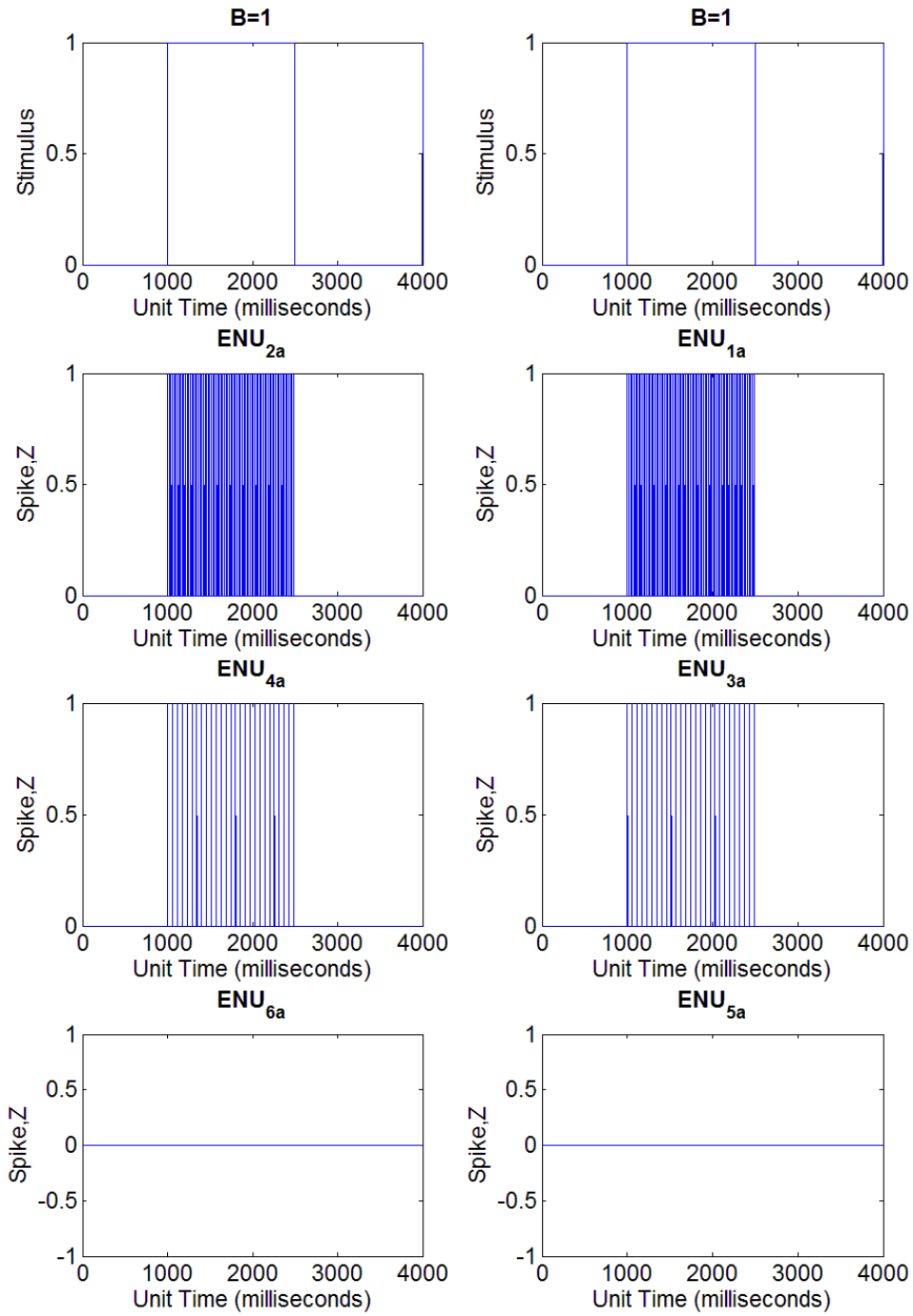

Figure 3.5. Output traces of E-DN in Figure 3.4 (inset) with just B-stimulus showing no spikes in corresponding ENU of fifth and sixth nodes (Eck5 & Eck6).

ENU PART			E-DN Node			
			1 or 2	3 or 4	5 or 6	
			ENU Group			
			ENU_1 or ENU_2	ENU_3 or ENU_4	ENU_5 or ENU_6	
			Basic ENU			
			ENU_{1a} or ENU_{2a}	ENU_{3a} or ENU_{4a}	ENU_{5a} or ENU_{6a}	
Dendrite	Linking Field	w_{lf}	No linking field			
		τ_{lf}				
	Feeding Field	w_{ff}	5	5	$5^{(+)}$	$5^{(-)}$
		τ_{ff}	10	10	$10^{(+)}$	$10^{(-)}$
Soma		τ_{pg}	7.5	7.5	7.5	
		V_{pg}	50	50	50	
		θ_o	0.5	0.5	0.5	

Table 3.1. Parameters used for the simulation (Fig. 3.5) of E-DN architecture shown in Figure 3.4. Parameter values with superscript (+) and (-) indicate values for excitatory and inhibitory connections respectively. Connections for parameter values without any superscript are excitatory by default.

The next step is to replicate the property of G-DN during both drive (D) and bias (B) inputs as shown in Figure 3.6. Unlike the case with just B-input (Fig. 3.1 & 3.2) node x1 receives stronger input stimulus due to the additional D-input and hence stronger stimulus is applied from x3 to x5 (than x4 to x6) with stronger inhibition from x3 to x6 (than x4 to x5) resulting in activity in x5 node but not in x6 (Fig. 3.7). In addition as soon as the network does not get D-input (but continues to receive B-input) there is activity in x6 node for a very short duration before the equally strong inputs from x3 and x4 cancel each other causing no activity in x5 and x6 nodes. Due to the elastic phenomenon of x6 node just described this property of G-DN is also called rebound/elastic property. The mechanics behind the cause is the short-term memory (psychological moment) property of G-DN given by the equation of z1 and z2 described earlier (Chapter-2, p22-26).

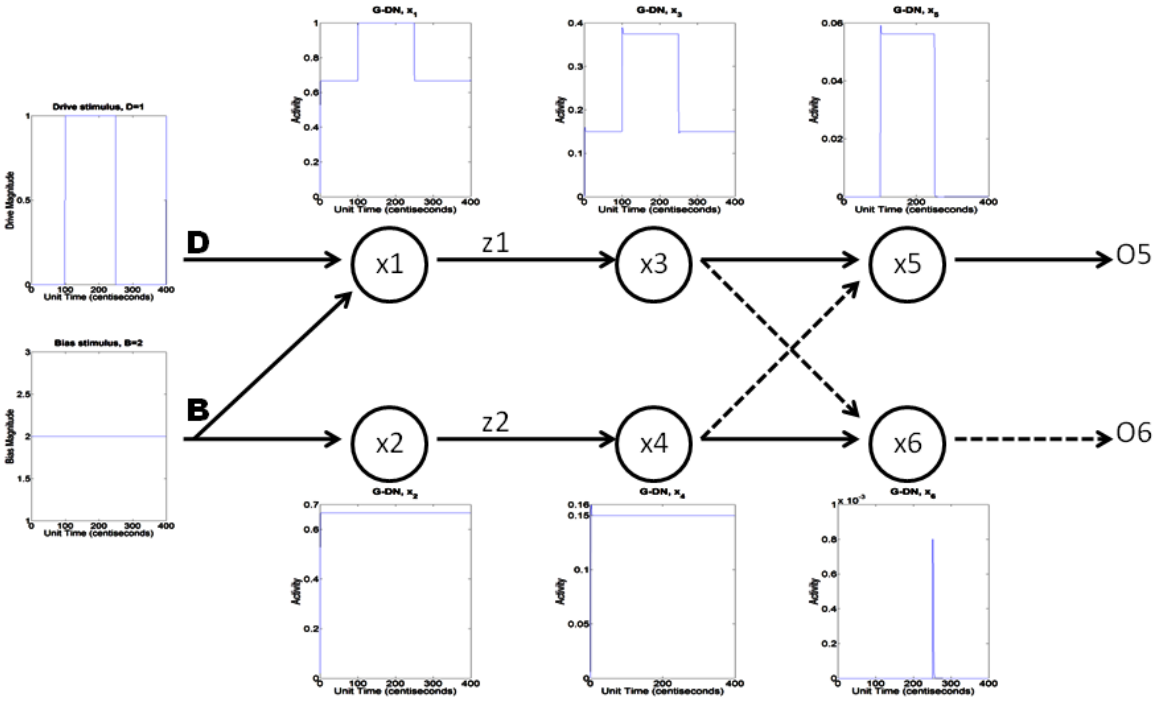

Figure 3.6. G-DN receiving both bias (B) and drive (D) stimulus.

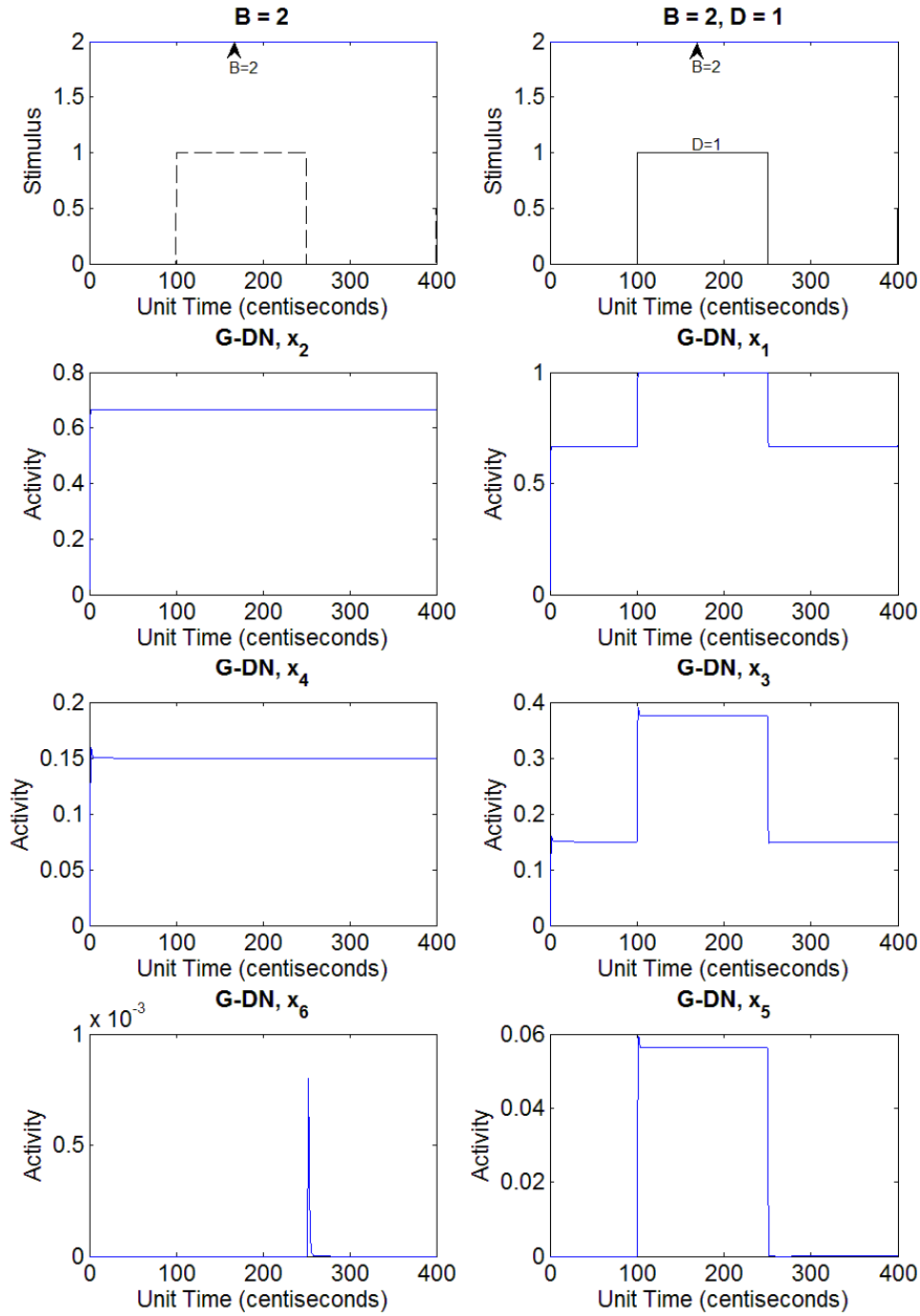

Figure 3.7. Output traces of G-DN in Figure 3.6 (inset) receiving both B and D-stimulus showing activity in node-5 (x_5) during B & D interval and activity in node-6 (x_6) for very short duration just after D-stimulus is turned off. Note that the dashed line (left stimulus/top plot) indicates absence of D-stimulus for node-2 during the interval node-1 receives D-stimulus.

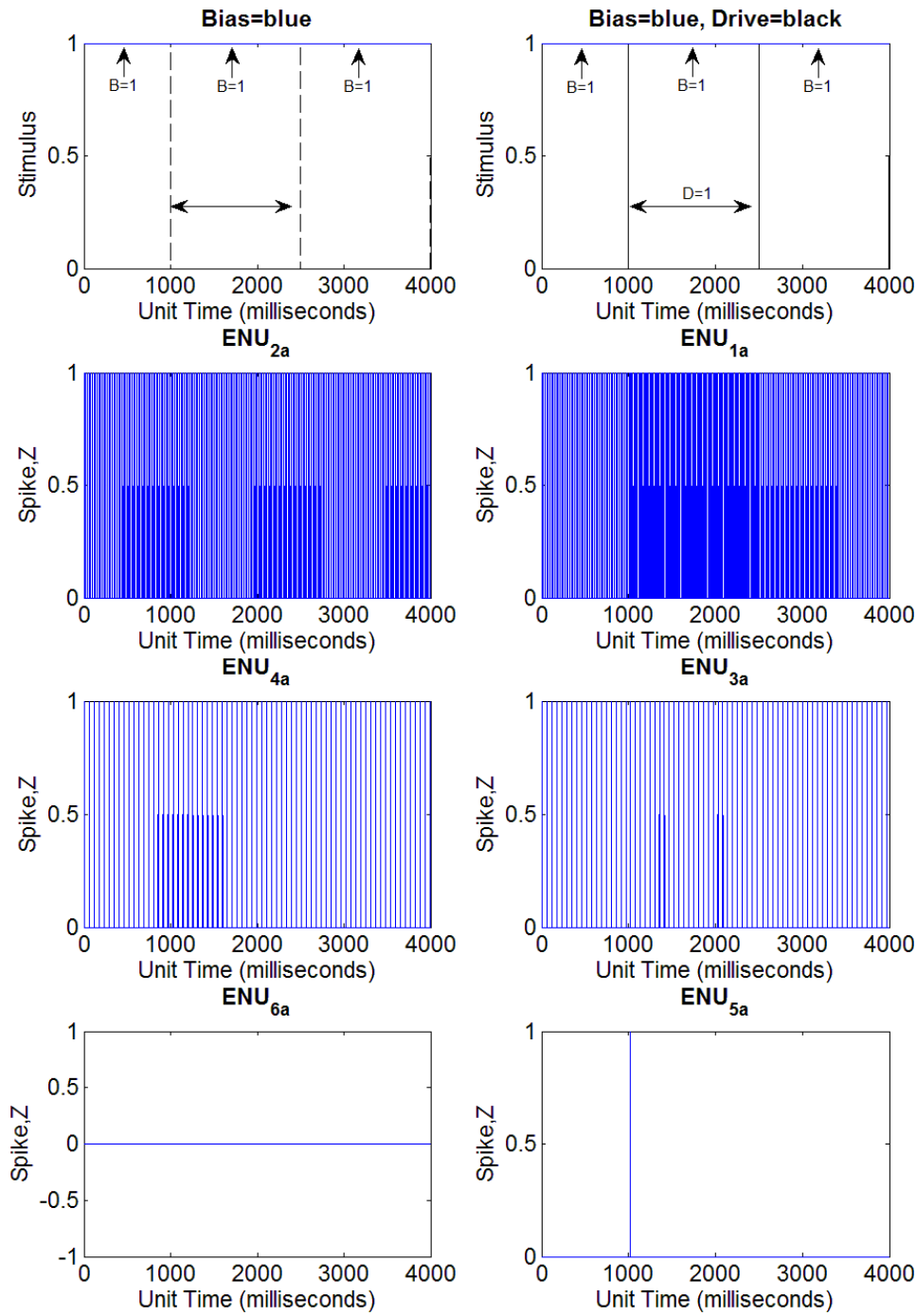

Figure 3.8. Output traces of E-DN architecture in Figure 3.4 but with both B and D-stimulus. Note that the dashed line (left stimulus/top plot) indicates absence of D-stimulus for node-2 (Eck2) during the interval node-1 (Eck1) receives D-stimulus.

Putting the E-DN seen in Figure 3.4 with the same parameters (table 3.1) through both B and D-stimulus produces the spike output traces shown in Figure 3.8. The

designed E-DN does not replicate the property of G-DN (Fig. 3.6 & 3.7). Apart for one spike in node-5 (Eck5) during the B & D interval there is no spiking even though node-1 (Eck1) clearly has more spiking during this interval. The increased spiking in the node-1 (Eck1) does not seem sufficient to considerably increase the spiking in node-3 (Eck3) relative to those during just B-stimulus. Hence the outcome is similar to the output trace with just B-stimulus (Fig. 3.5).

Adding more basic ENU's

The lack of change (Fig. 3.8) in node-3 (Eck3) even after receiving greater spiking input relative to node-4 (Eck4) could either be due to insufficient number of basic ENU's implemented in the E-DN or different to the parameter values or to the nature of PCNN dynamics. This section investigates the failure mechanism.

Using the same parameter values (table 3.1 with additional linking field parameters; $w_{lf} = 0.5$ & $\tau_{lf} = 1$), the basic ENU's in each node were increased by one, i.e., ENU_{xi} where i = a & b (Fig. 3.9). Running the simulation of the E-DN with increased number of basic ENU receiving both B and D-stimulus, the output trace of Figure 3.12 was obtained. With this network spikes now occur in both node-5 (Eck5) and node-6 (Eck6) during the B & D interval after which node-5 (Eck5) continues spiking. However this is not the behavior replicating G-DN (Fig. 3.6 & 3.7). Output trace of node-3 (Eck3) shows that though it is now receiving more input stimulus spikes (than E-DN in Fig. 3.8) spike output from this node does not increase proportionately. However the spiking pattern of node-3 (Eck3) is changed relative to node-4 (Eck4) causing successful inhibition (no spike) by either of the nodes (on respective Eck5 or Eck6) only at certain intervals.

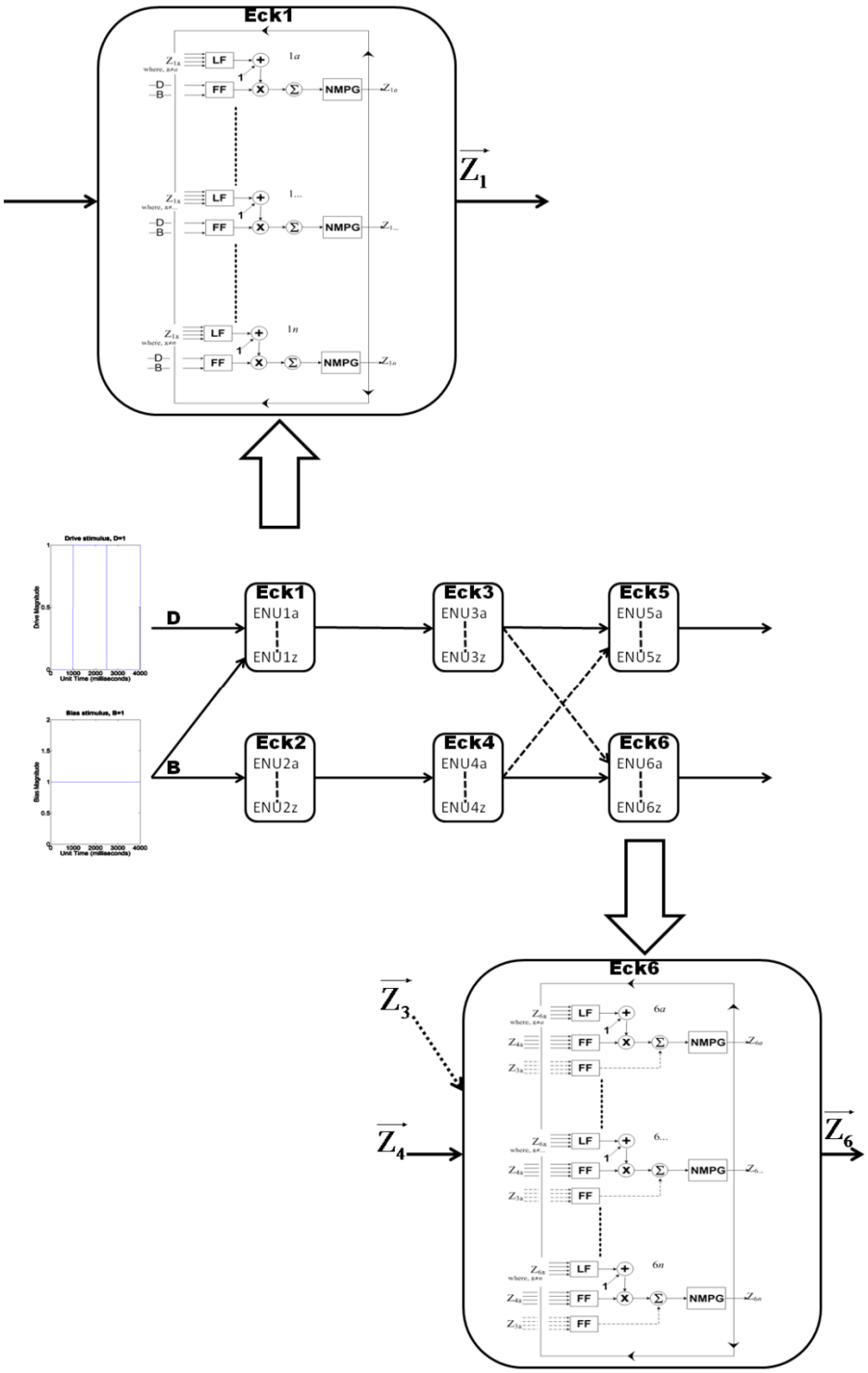

Figure 3.9. General scheme of E-DN for Figures 3.12, 3.13 and 3.15. This E-DN is similar to Figure 3.4 but with increased number of basic ENU's (a,…,z per ENU group, i.e., a to z basic ENU's) receiving both B & D-stimulus. The inset shows connection amongst basic ENU's within respective ENU group (ENU_1 & ENU_6 shown of nodes-1(Eck1) and node-6 (Eck6) respectively). Figures 3.10 and 3.11 provide enlarged views of the inset.

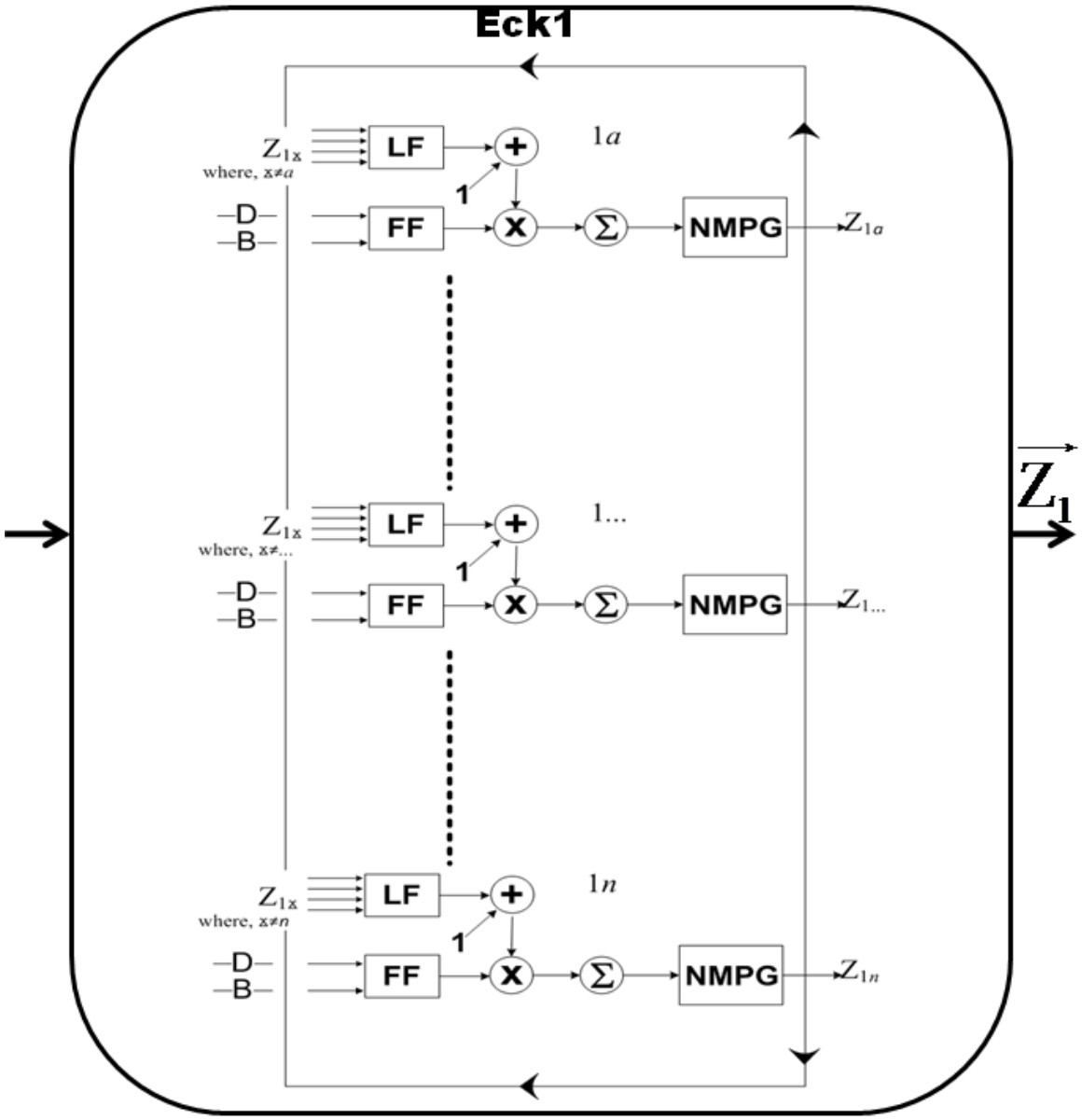

Figure 3.10. Enlarged view of the top inset seen in Figure 3.9 showing the configuration of *n*-basic ENU's within node-1 (Eck1). For i^{th} basic ENU its linking field (LF) receives output from neighboring basic ENU's apart from its own Z_{1i}, that is, elements of the LF input vector are the NMPG outputs excluding its own NMPG output it feeds into. But feeding field (FF) for all basic ENU's receives input stimulus which in the case of node-1 (Eck1) is the drive (D) and bias (B) stimulus as DC.

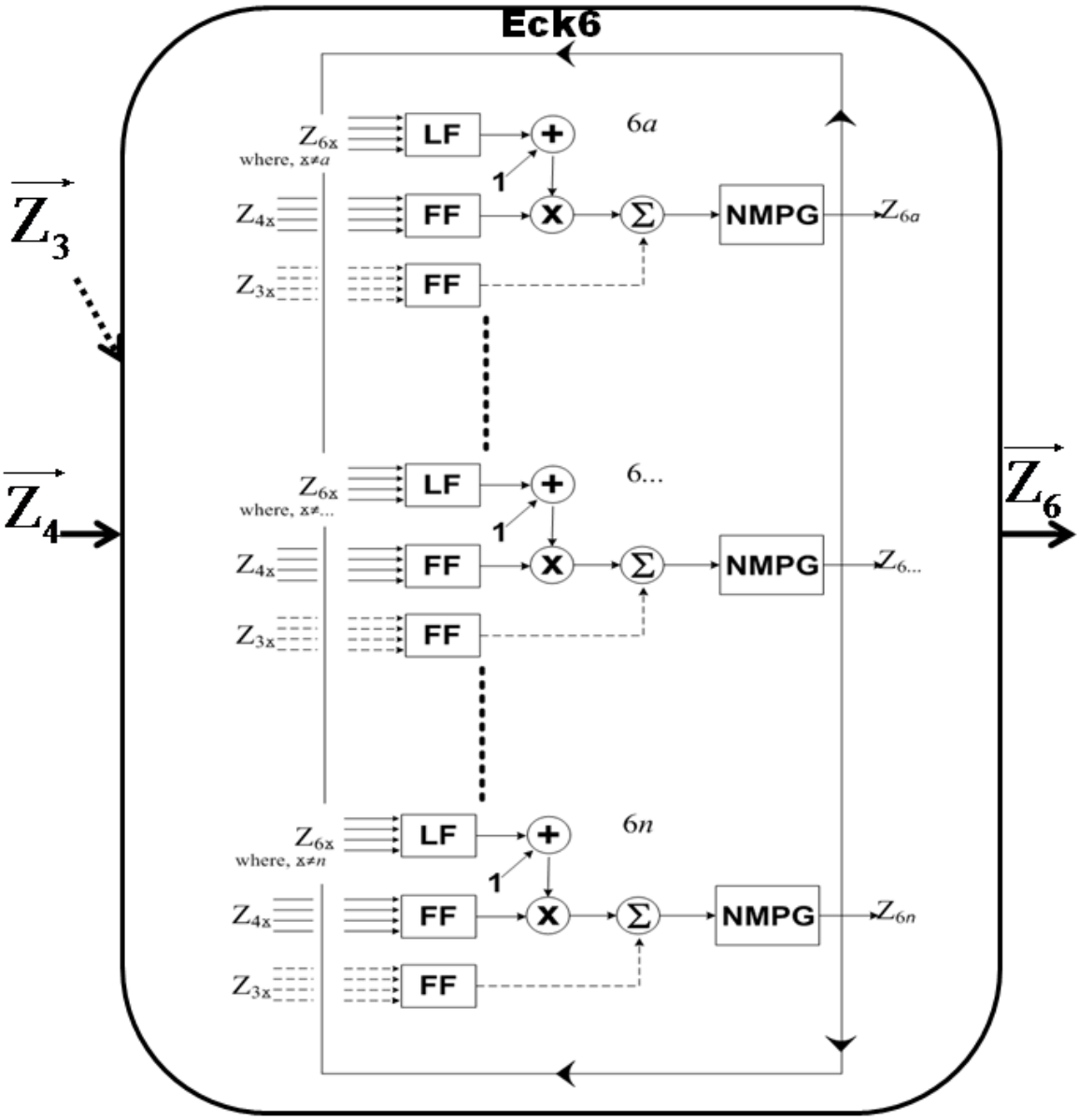

Figure 3.11. Enlarged view of the bottom inset (Fig. 3.9), showing the configuration of *n*-basic ENU's within node-6 (Eck6). Feeding fields (FF) for basic ENU's within Eck6 receives excitatory input (solid line) from Eck4 outputs ($\vec{Z}_4$) and inhibitory input (dashed line) from Eck3 outputs ($\vec{Z}_3$) via respective dendrites. Note that this is reversed for Eck5.

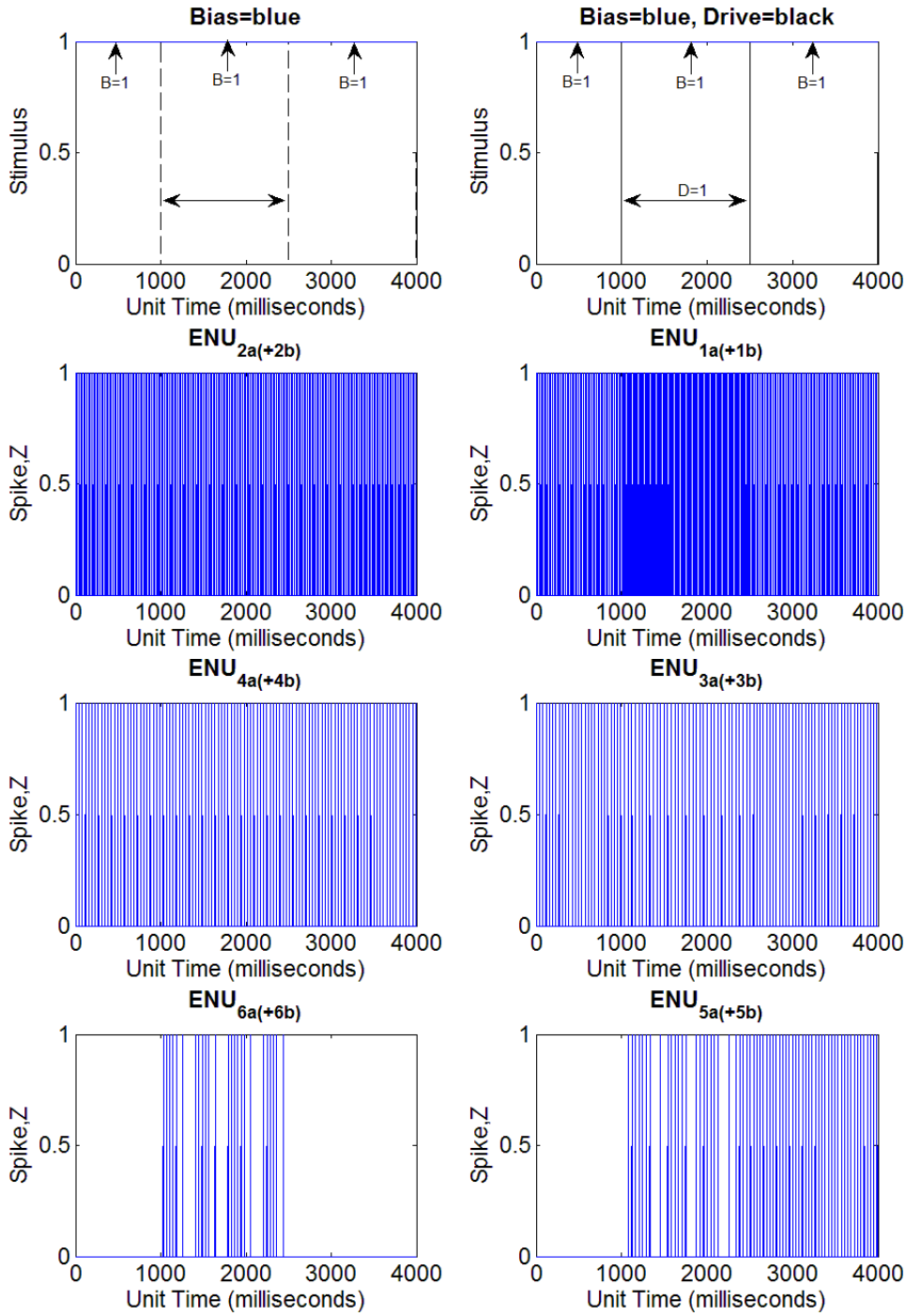

Figure 3.12. Output traces of just one basic ENU (ENU_{xa}) implemented (out of two per ENU group) in E-DN architecture of Figure 3.9 receiving both B and D-stimulus using parameters (table 3.1 with additional linking field parameters; $w_{lf} = 0.5$ & $\tau_{lf} = 1$).

Comparing Figure 3.12 to 3.8, spiking from Eck3 and Eck4 has increased which has resulted in Eck5 spiking during dual-stimuli, but so does Eck6. After the dual-stimuli, Eck5 continues to spike and not spiking from Eck6. Due to the lack of apparent increase in Eck3 spiking relative to Eck4 (Fig. 3.12) during dual-stimuli, the number of basic ENU's was increased using the same E-DN architecture (Fig. 3.9). The number of basic ENU's per group in E-DN (Fig. 3.12) was increased such that there are12 basic ENU's each in ENU_1 & ENU_2, 9 each in ENU_3 & ENU_4 and 3 each in ENU_5 & ENU_6 group. In addition, linking field parameter values were changed (from table 3.1) as shown in table 3.2. Output traces of this E-DN when run under simulation with both B and D-stimulus is shown in Figure 3.13.

ENU PART			**E-DN Node**		
			1 or 2	3 or 4	5 or 6
			ENU Group		
			ENU_1 or ENU_2	ENU_3 or ENU_4	ENU_5 or ENU_6
			Basic ENU		
			$ENU_{1a(b,\ldots,l)}$ or $ENU_{2a(b,\ldots,l)}$	$ENU_{3a(b,\ldots,i)}$ or $ENU_{4a(b,\ldots,i)}$	$ENU_{5a(b,c)}$ or $ENU_{6a(b,c)}$
Dendrite	Linking Field	w_{lf}	0.5	0.05	0.005
		τ_{lf}	1	1	1

Table 3.2. Parameters used for the simulation (Fig. 3.13) of E-DN architecture shown in Figure 3.9. All other parameter values (soma parameters) are same as in table 3.1.

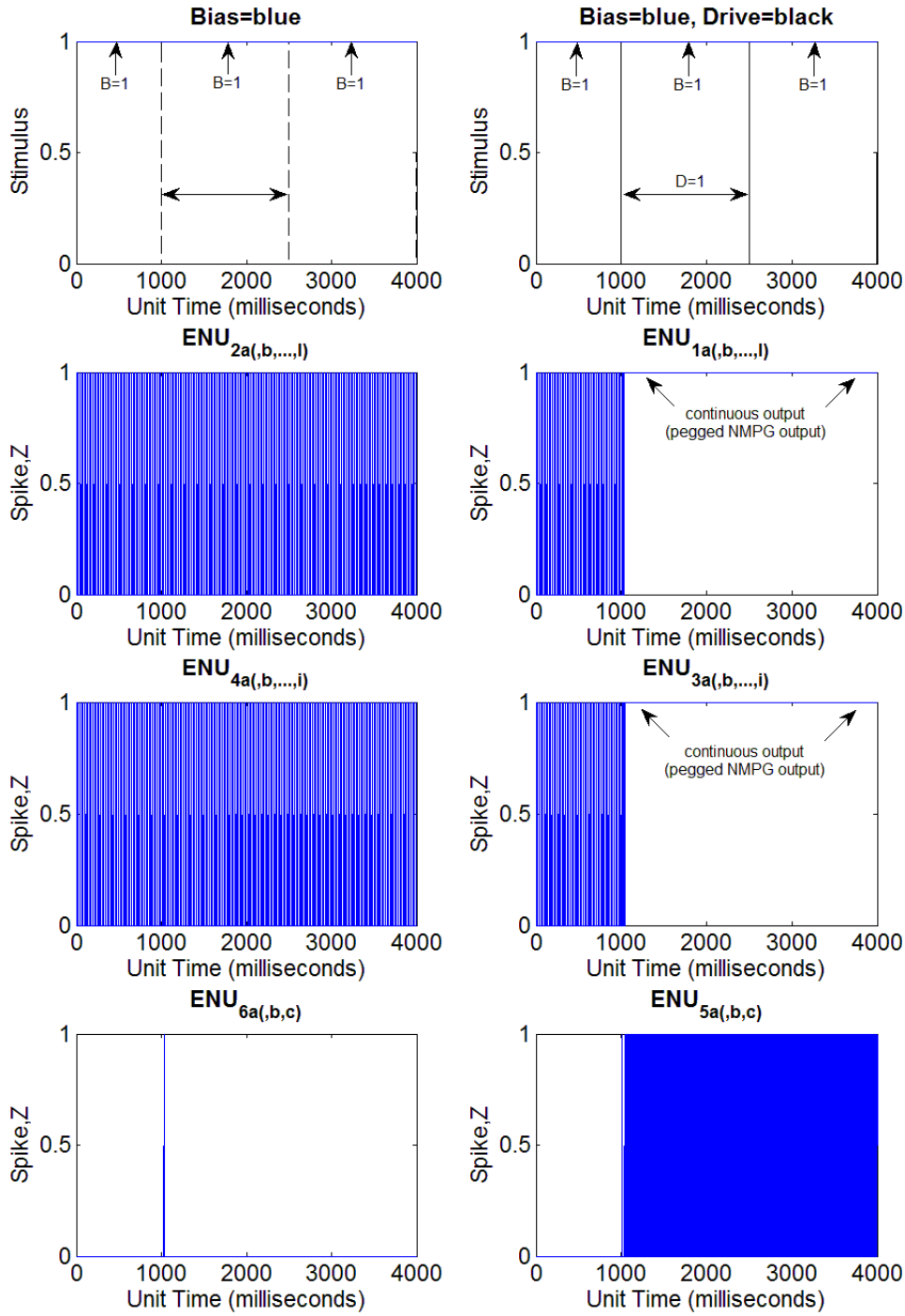

Figure 3.13. Output traces of just one basic ENU (ENU_{xa}) implemented (out of 12 each in ENU_1 & ENU_2, 9 each in ENU_3 & ENU_4 and 3 each in ENU_5 & ENU_6 group) in E-DN architecture of Figure 3.9 receiving both B and D-stimulus using parameters (table 3.2).

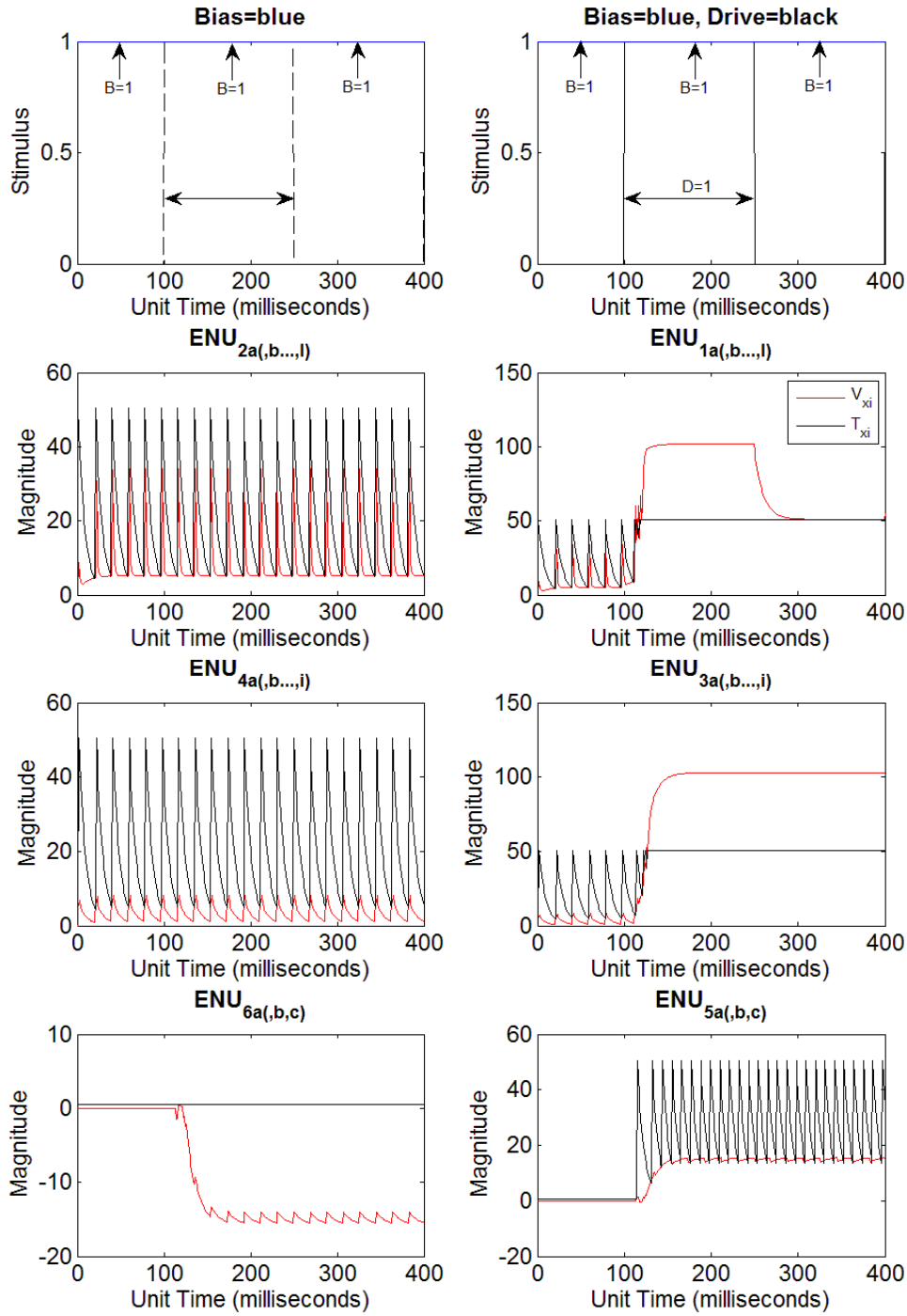

Figure 3.14. Soma inputs compared with soma threshold for the traces seen in Figure 3.13. V_{xi} (red) soma input and T_{xi} (black) soma threshold (or θ_{xi}). Notations as used in Figure 3.3. Note that after initiating dual stimuli (B & D), the T_{xi} (or θ_{xi}) for Eck1, Eck3 and Eck5 never reaches its resting baseline ($\theta_o = 0.5$, from table 3.1) unlike their counterparts (Eck2, Eck4 and Eck6). Thus ENU's in the former three nodes are firing in saturated mode.

Output traces (Fig. 3.13) of the current E-DN shows spiking in Eck5 while spiking in Eck6 is inhibited during B & D-stimulus interval. This should be the case (unlike those seen in Fig. 3.8 & 3.12) since Eck5 receives pulsed inputs from nodes receiving B & D-stimulus while preceding nodes for Eck6 receives only B-stimulus. But after the B & D-stimulus interval there is no spiking from Eck6 (that is, no elasticity) and instead Eck5 spiking persists.

The outputs from Eck1, Eck3 and Eck4 indicate that their respective ENU's are firing in saturated mode as shown in Figure 3.14. Apart from the linking field parameters (whose purpose is synchronization) all other parameters are the same as table 3.1. Hence increased spiking is due to considerable increase in basic ENU numbers particularly in first four nodes of E-DN. ENU's in saturated mode is not desired for E-DN because the network cannot replicate G-DN as one connection of nodes (those receiving B & D-stimulus) will uniformly be having an upper hand, incapable of producing any dipole property.

Next the number of basic ENU's per group in E-DN architecture (Fig. 3.9) is changed (decreased relative to Fig. 3.13), such that there are12 basic ENU's each in ENU_1 & ENU_2, 3 each in ENU_3 & ENU_4 and 3 each in ENU_5 & ENU_6 groups. In addition, different parameter values are used for this E-DN (table 3.3). A major change in parameter value is the time constant of inhibitory feeding field which is set larger than the corresponding value of the excitatory dendrite within respective ENU_x group. Output traces of this E-DN when run under simulation with both B and D-stimulus are shown in Figure 3.15.

ENU PART			E-DN Node			
			1 or 2	3 or 4	5 or 6	
			ENU Group			
			ENU_1 or ENU_2	ENU_3 or ENU_4	ENU_5 or ENU_6	
			Basic ENU			
			$ENU_{1a(b,\ldots,l)}$ or $ENU_{2a(b,\ldots,l)}$	$ENU_{3a(b,c)}$ or $ENU_{4a(b,c)}$	$ENU_{5a(b,c)}$ or $ENU_{6a(b,c)}$	
Dendrite	Linking Field	w_{lf}	0.5	0.05	0.005	
		τ_{lf}	1	1	1	
	Feeding Field	w_{ff}	0.5	1	$5^{(+)}$	$5^{(-)}$
		τ_{ff}	10	10	$10^{(+)}$	$12.5^{(-)}$

Table 3.3. Parameters used for the simulation (Fig. 3.15) of E-DN architecture shown in Figure 3.9. Notice that the linking field parameter used for simulation in Figure 3.15 remains unchanged (compared to table 3.2 for Fig. 3.13 simulation) but the feeding field weight (w_{ff}) for nodes receiving the first line of stimulus (nodes 1 & 2) has changed (reduced to 0.5). Also the time constant for inhibitory feeding field is increased (12.5). The parameters for soma/neuromime remain the same as in table 3.1.

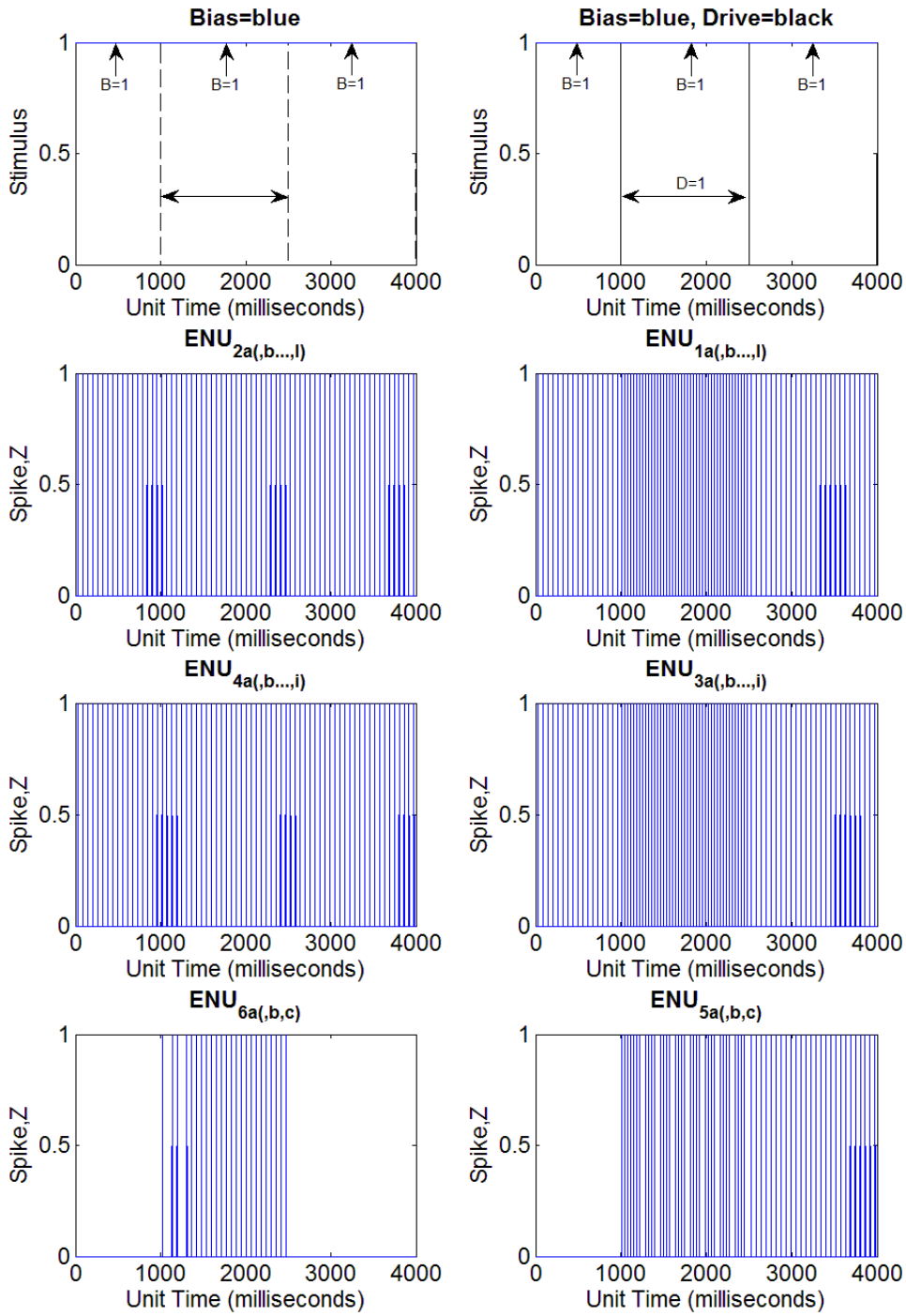

Figure 3.15. Output traces of one basic ENU (ENU_{xa}) implemented (out of 12 each in ENU_1 & ENU_2, 3 each in ENU_3 & ENU_4 and 3 each in ENU_5 & ENU_6 group) in E-DN architecture of figure 3.9 receiving both B and D-stimulus using parameters given in table 3.3.

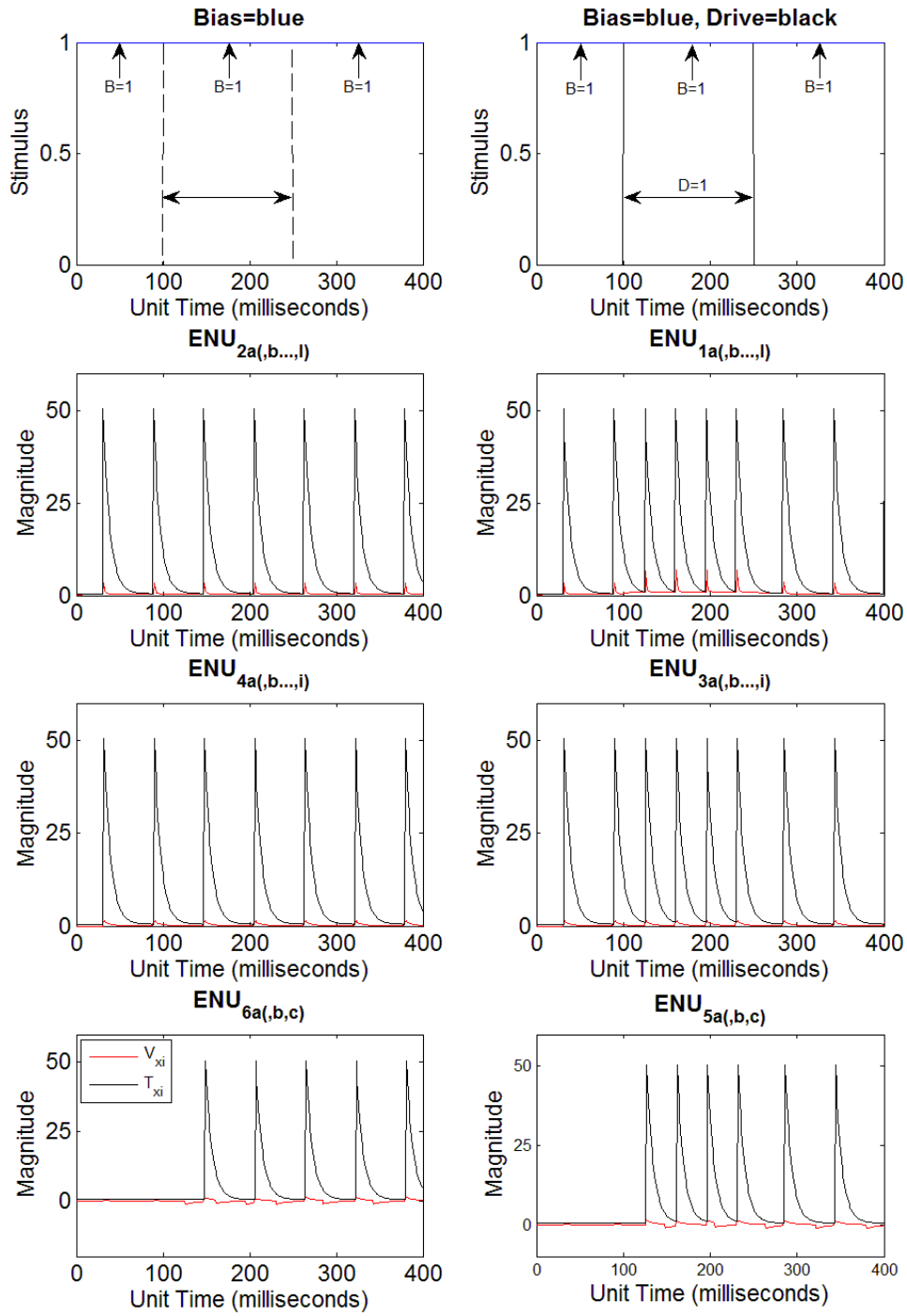

Figure 3.16. Soma inputs (V_{xi}, red) compared with soma threshold (T_{xi} or θ_{xi}, black) for the traces seen in Figure 3.15. V_{xi}, soma input and T_{xi}, soma threshold (or θ_{xi}). Notice that T_{xi} (or θ_{xi}) of all the ENU's in all six nodes reach their resting baseline ($\theta_o = 0.5$, from table 3.1).

The output traces in Figure 3.15 are qualitatively similar to those already seen in Figure 3.12 with respect to spiking from node-5 (Eck5) and node-6 (Eck6) of E-DN. However unlike Figure 3.12 there is a noticeable increase in node-3 (Eck3) spiking. The spiking behavior in the first four nodes (Eck1 to Eck4) corresponds intuitively with the initial stimulus node-1 (Eck1) and node-2 (Eck2) receives. To check the mode of the ENU's, soma inputs were compared with threshold as seen in Figure 3.16. The figure shows that the ENU's are no longer in saturated mode as was the case for earlier E-DN (Fig. 3.13).

Till now the network architecture of E-DN has been identical to G-DN, but the goal is to replicate the property of G-DN. While using G-DN as the roadmap network the E-DN architecture can be changed or modified to achieve the goal. The results just shown indicate that PCNN dynamics differ significantly enough to require this.

Two ENU groups within initial nodes (node-1 or Eck1 & node-2 or Eck2) with reciprocal inhibition (Eck3↔Eck6 & Eck4↔Eck5)

The previous E-DN (Fig. 3.15) has spikes from Eck6 during B and D-stimulus though Eck3 is spiking more than Eck4. Increasing just the basic ENU's can lead them into saturated mode but this particular problem of insufficient inhibition can be tackled by adding reciprocal inhibition between the nodes (Eck3 & Eck6 and Eck4 & Eck5). In addition, during B-stimulus (post dual stimuli) both Eck5 and Eck6 are at the end of network receiving the same B-stimulus but Eck5 continues spiking. To solve this issue two ENU groups (ENU_{1syn} & ENU_{2syn}) are introduced such that they receive pulsed inputs from ENU_1 & ENU_2 groups respectively with the intention to achieve certain

amount of synchrony in inputs, particularly during B-stimulus. The ENU_1 and ENU_{1syn} constitute Eck1 (similarly for Eck2). The new E-DN is shown in Figures 3.17 and 3.18.

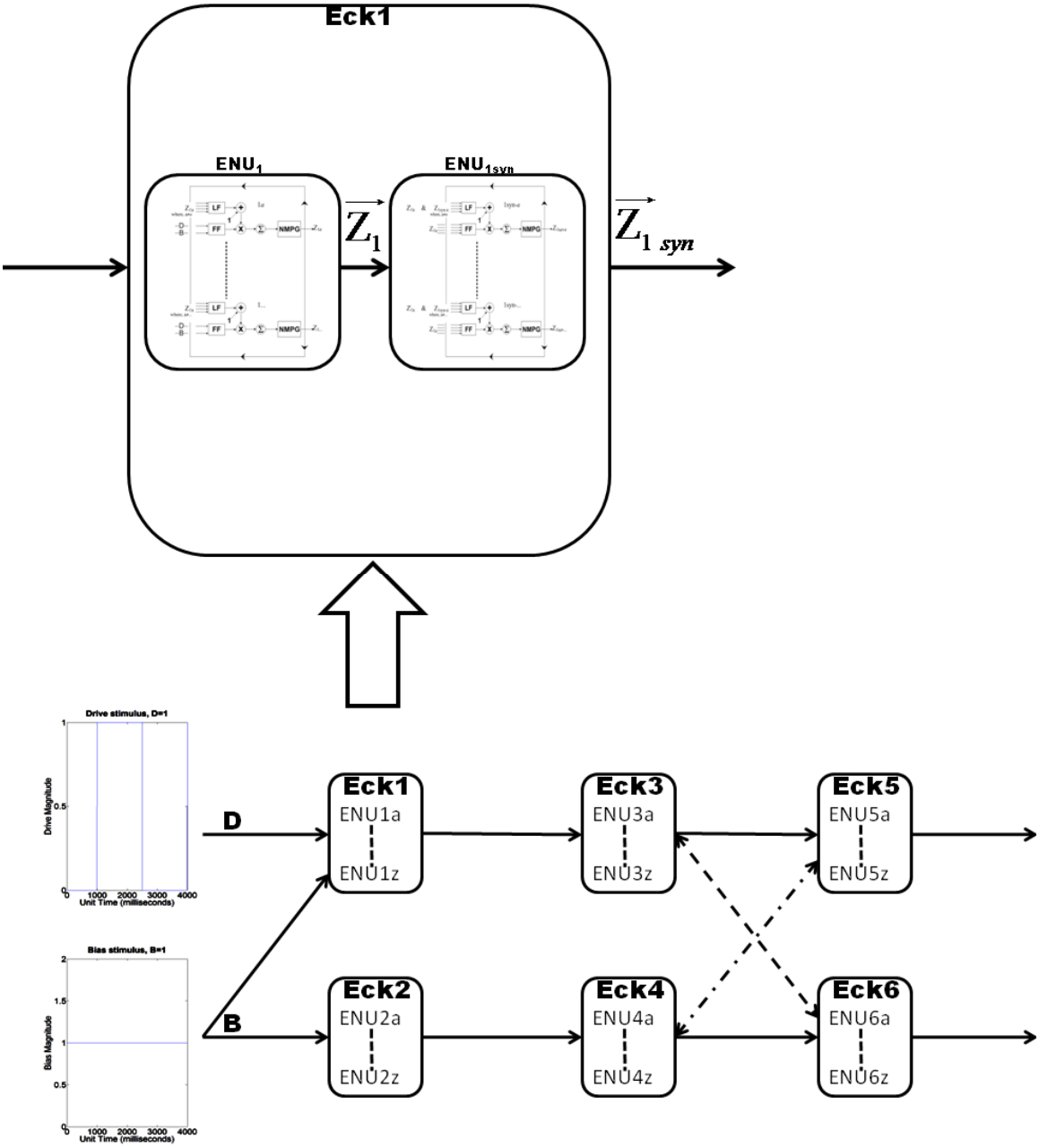

Figure 3.17. E-DN with reciprocal inhibition between nodes 3↔6 (Eck3↔Eck6) & 4↔5 (Eck4↔Eck5) with two ENU groups each in node-1 (ENU_1 & ENU_{1syn} in Eck1) & node-2 (ENU_2 & ENU_{2syn} in Eck2). Number of basic ENU's per ENU groups: 12 each in ENU_1 & ENU_2, 12 each in ENU_{1syn} & ENU_{2syn}; 9 each in ENU_3 & ENU_4, 3 each in ENU_5 & ENU_6.

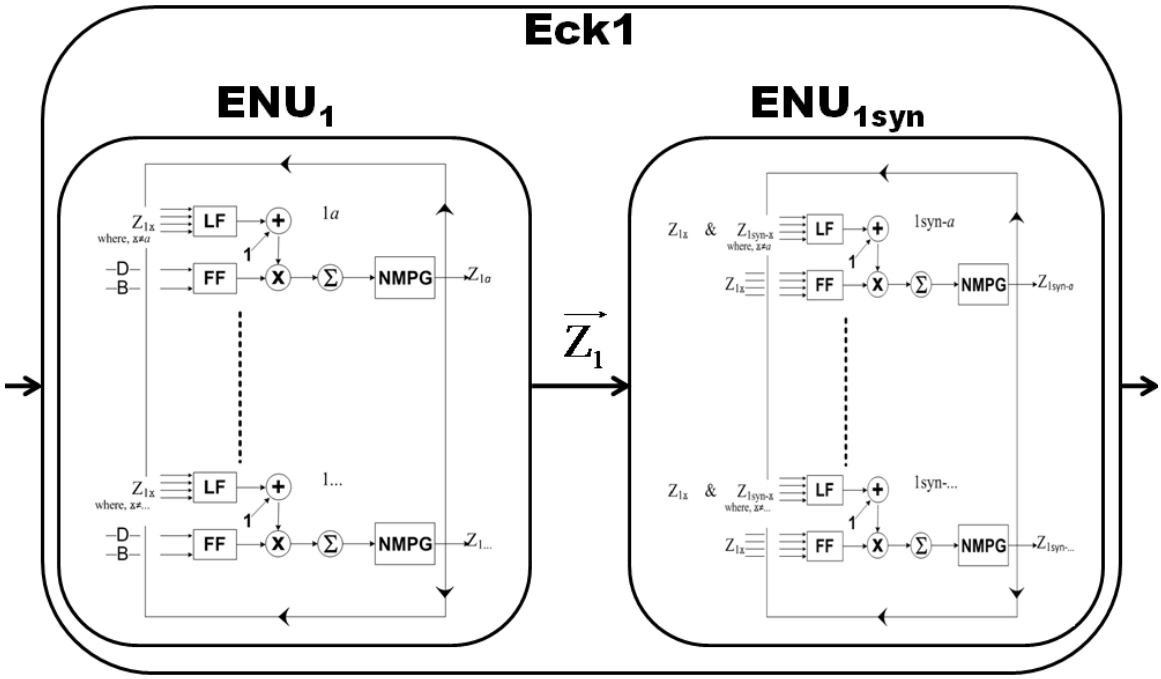

Figure 3.18. Enlarged view of the inset seen in Figure 3.17 showing the configuration of *n*-basic ENU's amongst the two ENU groups (ENU_1 & ENU_{1syn}) within Eck1. Feeding field (FF) for all basic ENU's within ENU_1 group receives input stimulus which in the case of Eck1 is the drive (D) and bias (B) stimulus as DC. However, outputs of ENU_1 group ($\vec{Z}_1$) are the inputs for the FF of basic ENU's within ENU_{1syn} group. Finally, inputs for Eck3 and Eck4 are from ENU_{1syn} ($\vec{Z}_{1syn}$) of Eck1 and ENU_{2syn} ($\vec{Z}_{2syn}$) of Eck2 respectively. Notice that LF's in ENU_{1syn} and ENU_{2syn} receives $\vec{Z}_1$ and $\vec{Z}_2$ respectively in addition to receiving NMPG outputs within ENU_{1syn} and ENU_{2syn}.

Output traces following simulation using parameters given in table 3.4 for E-DN (Fig. 3.17) are shown in Figure 3.19. The spiking from Eck5 and Eck6 resembles those seen in Figure 3.15. However amount of spiking from Eck6 during B and D-stimuli has decreased. Hence increasing the strength of inhibitory connections from basic ENU's of the preceding nodes (Eck3 for Eck6 and Eck4 for Eck5) could inhibit the Eck6 spiking. This was done by changing the inhibitory feeding field weight parameter for basic ENU's in Eck5 and Eck6 ($w_{ff} = 5^{(-)}$, increased from $w_{ff} = 2^{(-)}$). The output traces with increased inhibition is shown in Figure 3.20.

ENU PART			**E-DN Node**					
			1 or 2		3 or 4		5 or 6	
			ENU Group					
			ENU_1 or ENU_2	ENU_{1syn} or ENU_{2syn}	ENU_3 or ENU_4		ENU_5 or ENU_6	
			Basic ENU					
			$ENU_{1a(b,\ldots,l)}$ or $ENU_{2a(b,\ldots,l)}$	$ENU_{1syn\text{-}a(b,\ldots,l)}$ or $ENU_{2syn\text{-}a(b,\ldots,l)}$	$ENU_{3a(b,\ldots,i)}$ or $ENU_{4a(b,\ldots,i)}$		$ENU_{5a(b,\ldots,c)}$ or $ENU_{6a(b,\ldots,c)}$	
Dendrite	linking field	w_{lf}	0.5	0.5 (amongst ENU1syn-…) 1 (with ENU1…) (similarly for ENU2syn-…)	0.5		0.5	
		τ_{lf}	1	1	1		1	
	feeding field	w_{ff}	0.5	1	$1^{(+)}$	$5^{(-)}$	$2^{(+)}$	$2^{(-)}$
		τ_{ff}	10	10	$10^{(+)}$	$30^{(-)}$	$20^{(+)}$	$20^{(-)}$

Table 3.4. Parameters used for the simulation (Figure 3.19) of E-DN architecture shown in Figure 3.17. Notice that the linking field parameter weight (w_{lf}) for ENU_{1syn} & ENU_{2syn} is such that $w_{lf} = 0.5$ between $ENU_{1syn\text{-}\ldots}$'s & between $ENU_{2syn\text{-}\ldots}$'s while $w_{lf} = 1$ between $ENU_{1\ldots}$'s & between $ENU_{2\ldots}$'s. The parameters for soma/neuromime remain the same as in table 3.1.

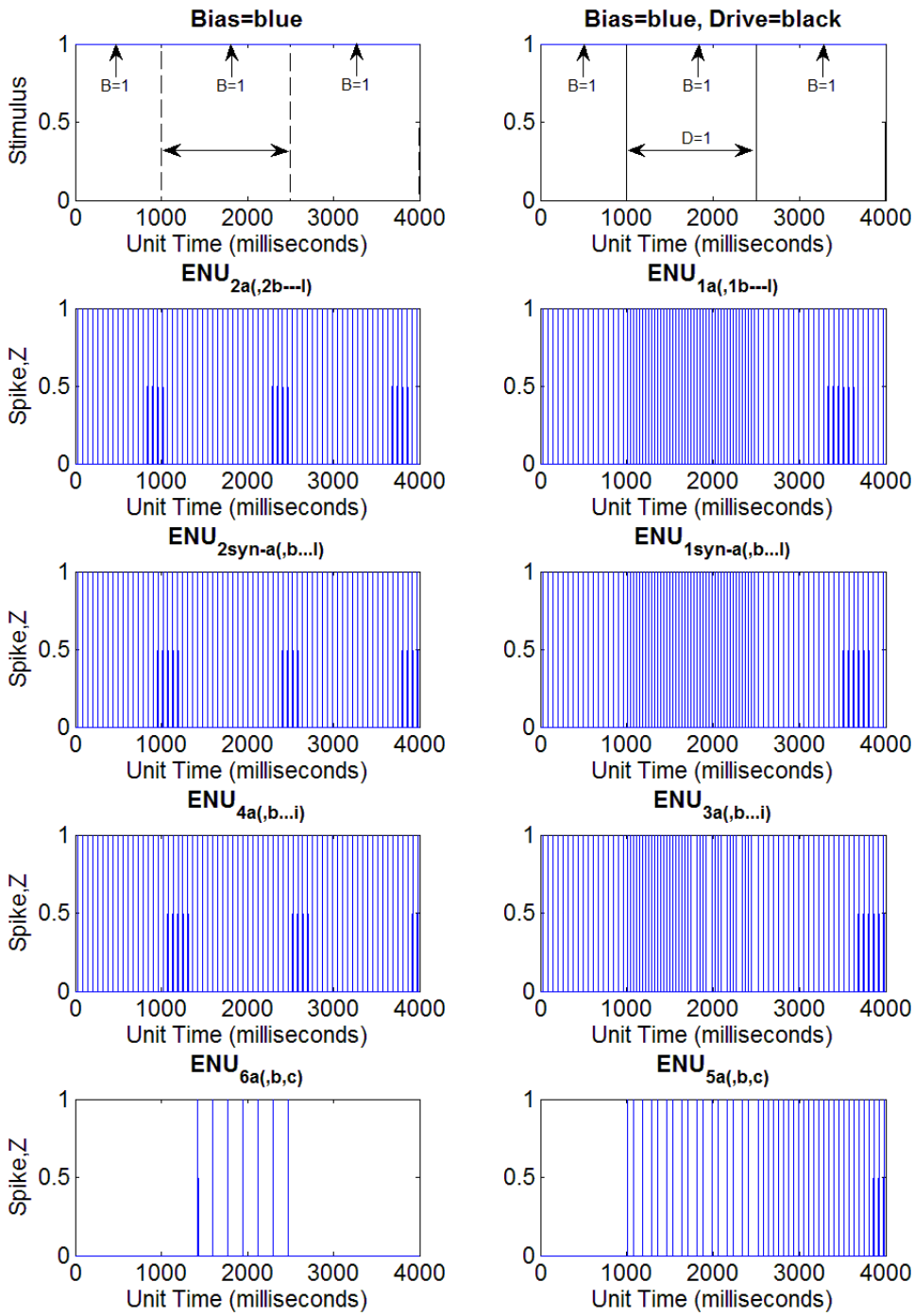

Figure 3.19. Output traces of one basic ENU (ENU_{xa}) implemented (out of 12 each in ENU_1 & ENU_2, 12 each in ENU_{1syn} & ENU_{2syn}, 9 each in ENU_3 & ENU_4 and 3 each in ENU_5 & ENU_6 group) in E-DN architecture of Figure 3.17 receiving both B and D-stimulus using parameters given in table 3.4.

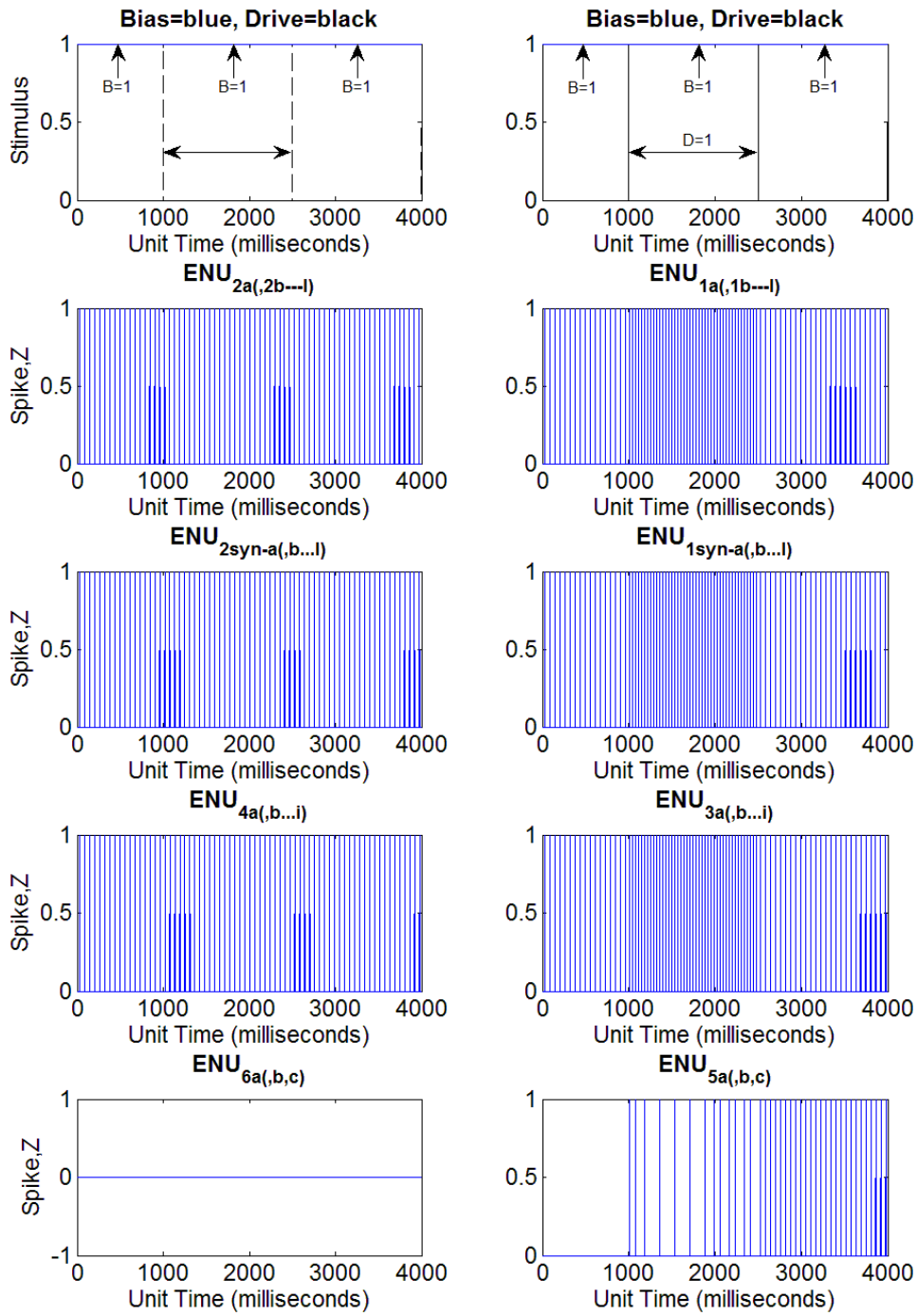

Figure 3.20. Output traces of just basic ENU (ENU_{xa}) implemented (out of 12 each in ENU_1 & ENU_2, 12 each in ENU_{1syn} & ENU_{2syn}, 9 each in ENU_3 & ENU_4 and 3 each in ENU_5 & ENU_6 group) in E-DN architecture of Figure 3.17 receiving both B and D-stimulus using same parameters as in table 3.4 with the exception that $w_{ff} = 5^{(-)}$ for basic $ENU_{5a(b,c)}$ or $ENU_{6a(b,c)}$,i.e., feeding field weights for incoming cross-inhibitions.

The reciprocal inhibition with forward and backward component in the E-DN is not successful in reproducing the property of G-DN (Fig. 3.19 & 3.20). During initial B-stimulus the forward inhibition (Eck3$\rightarrow^{(-)}$Eck6 & Eck4$\rightarrow^{(-)}$Eck5) is strong enough to prevent spiking. With B & D-stimulus, Eck6 receives stronger inhibition leading to no backward inhibition of Eck3 which in turn makes Eck3 stimulate Eck5 consistently (Fig. 3.20). However spiking in Eck5 continues after the dual stimuli and no elastic property is obtained.

Three ENU groups within initial nodes (node-1 or Eck1 & node-2 or Eck2) without reciprocal inhibition

The architecture of E-DN in Figure 3.17 was next modified by removing the backward inhibition (Eck3$^{(-)}\leftarrow$Eck6 and Eck4$^{(-)}\leftarrow$Eck5). Spiking from the middle two nodes (Eck3 & Eck4) is to be reduced while still maintaining the desired relation with B, D-stimulus. That is, Eck3 is to have relatively more spiking than Eck4. To achieve this, two more ENU groups (ENU_{1elas} & ENU_{2elas}) are introduced into the first two nodes (Eck1 & Eck2) such that they receive pulsed inputs from ENU_{1syn} & ENU_{2syn} respectively but project lateral inhibition to these groups (Fig. 3.21 & 3.22).

Simulation results (Fig. 3.23) show that the E-DN of Figure 3.21 has achieved one property of G-DN, i.e., during B & D-stimulus Eck3 is able to excite Eck5 despite receiving inhibition from Eck4, whereas during B-stimulus (pre- or post-dual stimuli) the equal strength of excitation and inhibition causes no spiking in either Eck5 or Eck6. However unlike G-DN (Fig. 3.6 & 3.7) no spiking occurs in Eck6 just after the removal of D-stimulus. In other words, rebound/elastic property of G-DN is still not represented

by the current E-DN.

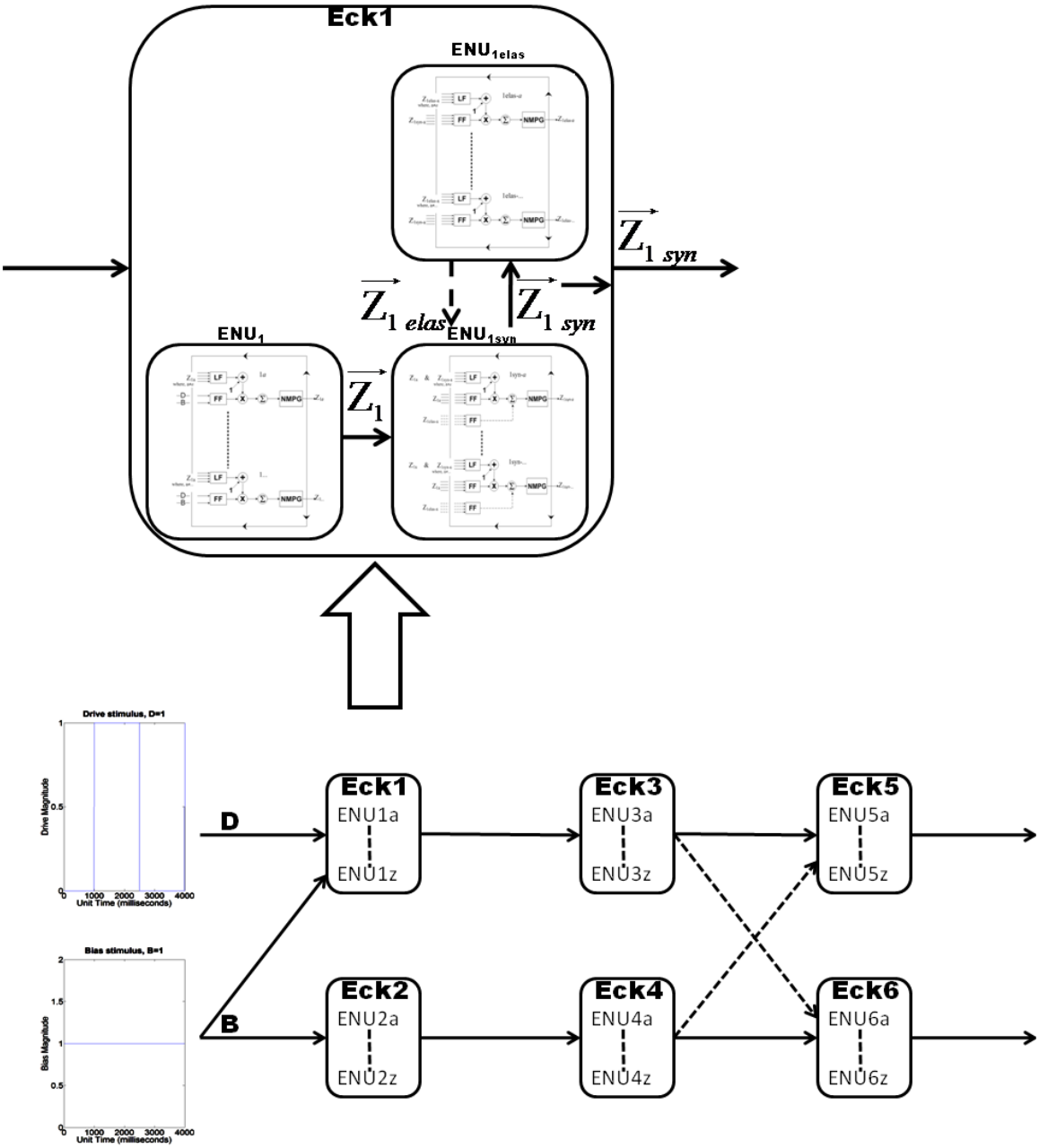

Figure 3.21. E-DN with three ENU groups (ENU_1, ENU_{1syn} & ENU_{1elas}) in Eck1 (and Eck2) such that ENU_{1elas} receives pulsed inputs and sends inhibitory pulses back to ENU_{1syn}. Number of basic ENU's per ENU groups: 12 each in ENU_1 & ENU_2, 6 each in ENU_{1syn} & ENU_{2syn}, 12 each in ENU_{1elas} & ENU_{2elas}; 12 each in ENU_3 & ENU_4 and 12 each in ENU_5 & ENU_6.

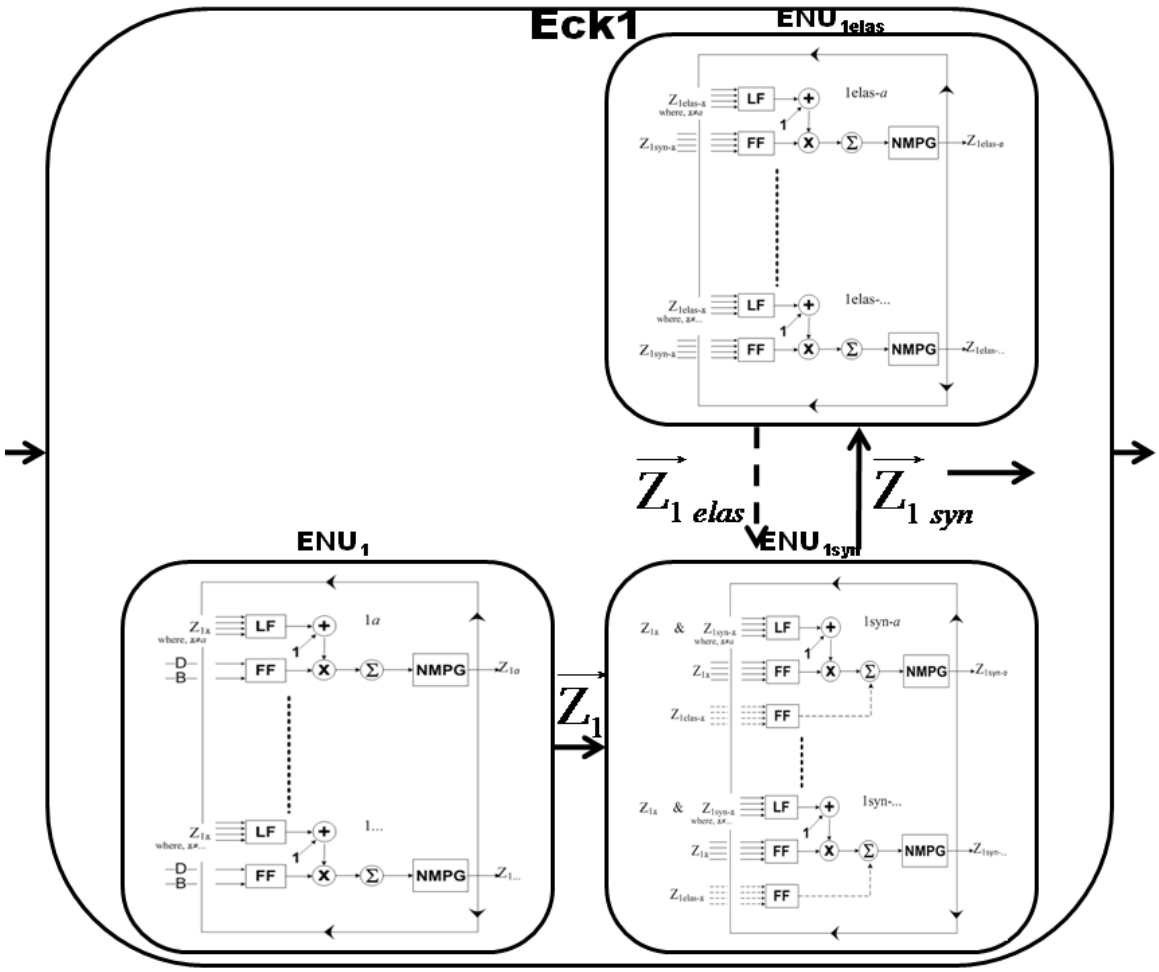

Figure 3.22. Enlarged view of the inset seen in Figure 3.21 showing the configuration of *n*-basic ENU's amongst the three ENU groups (ENU_1, ENU_{1syn} & ENU_{1elas}) within Eck1.

Feeding field (FF) for all basic ENU's within ENU_1 group receives input stimulus which in the case of Eck1 is the drive (D) and bias (B) stimulus as DC. However, outputs of ENU_1 group ($\vec{Z}_1$) are the inputs for the FF (excitatory) of basic ENU's within ENU_{1syn} group whose outputs ($\vec{Z}_{1syn}$) in turn are the inputs for the FF of basic ENU's within ENU_{1elas} group. The ENU_{1elas} outputs ($\vec{Z}_{1elas}$) are then inputs for the FF of inhibitory dendrite of ENU_{1syn} (i.e., lateral inhibition).

Finally, inputs for Eck3 and Eck4 are from ENU_{1syn} ($\vec{Z}_{1syn}$) of Eck1 and ENU_{2syn} ($\vec{Z}_{2syn}$) of Eck2 respectively.

ENU Part Dend.		**E-DN Node**						
		1 or 2				3 or 4	5 or 6	
		ENU Group						
		ENU_1 or ENU_2	ENU_{1syn} or ENU_{2syn}		ENU_{1elas} or ENU_{2elas}	ENU_3 or ENU_4	ENU_5 or ENU_6	
		Basic ENU						
		$ENU_{1a(b,\ldots,l)}$ or $ENU_{2a(b,\ldots,l)}$	$ENU_{1syn\text{-}a(b,\ldots,f)}$ or $ENU_{2syn\text{-}a(b,\ldots,f)}$		$ENU_{1elas\text{-}a(b,\ldots,l)}$ or $ENU_{2elas\text{-}a(b,\ldots,l)}$	$ENU_{3a(b,\ldots,l)}$ or $ENU_{4a(b,\ldots,l)}$	$ENU_{5a(b,\ldots,l)}$ or $ENU_{6a(b,\ldots,l)}$	
LF	w_{lf}	0.5	0.5		0.5	0.5	0.5	
	τ_{lf}	1	1		1	1	1	
FF	w_{ff}	0.5	$1^{(+)}$	$125^{(-)}$	1	$1^{(+)}$	$0.5^{(+)}$	$2^{(-)}$
	τ_{ff}	10	$10^{(+)}$	$30^{(-)}$	10	$10^{(+)}$	$10^{(+)}$	$40^{(-)}$

Table 3.5. Parameters used for simulation (Fig. 3.23) of E-DN architecture shown in Figure 3.21. Notice that the linking field parameter weight for ENU_{1syn} & ENU_{2syn}, w_{lf} = 0.5 between $ENU_{1syn\text{-}\ldots}$'s (& also between $ENU_{2syn\text{-}\ldots}$'s) and also with $ENU_{1\ldots}$'s (& with $ENU_{2\ldots}$'s). The parameters for soma/neuromime remain same as in table 3.1.

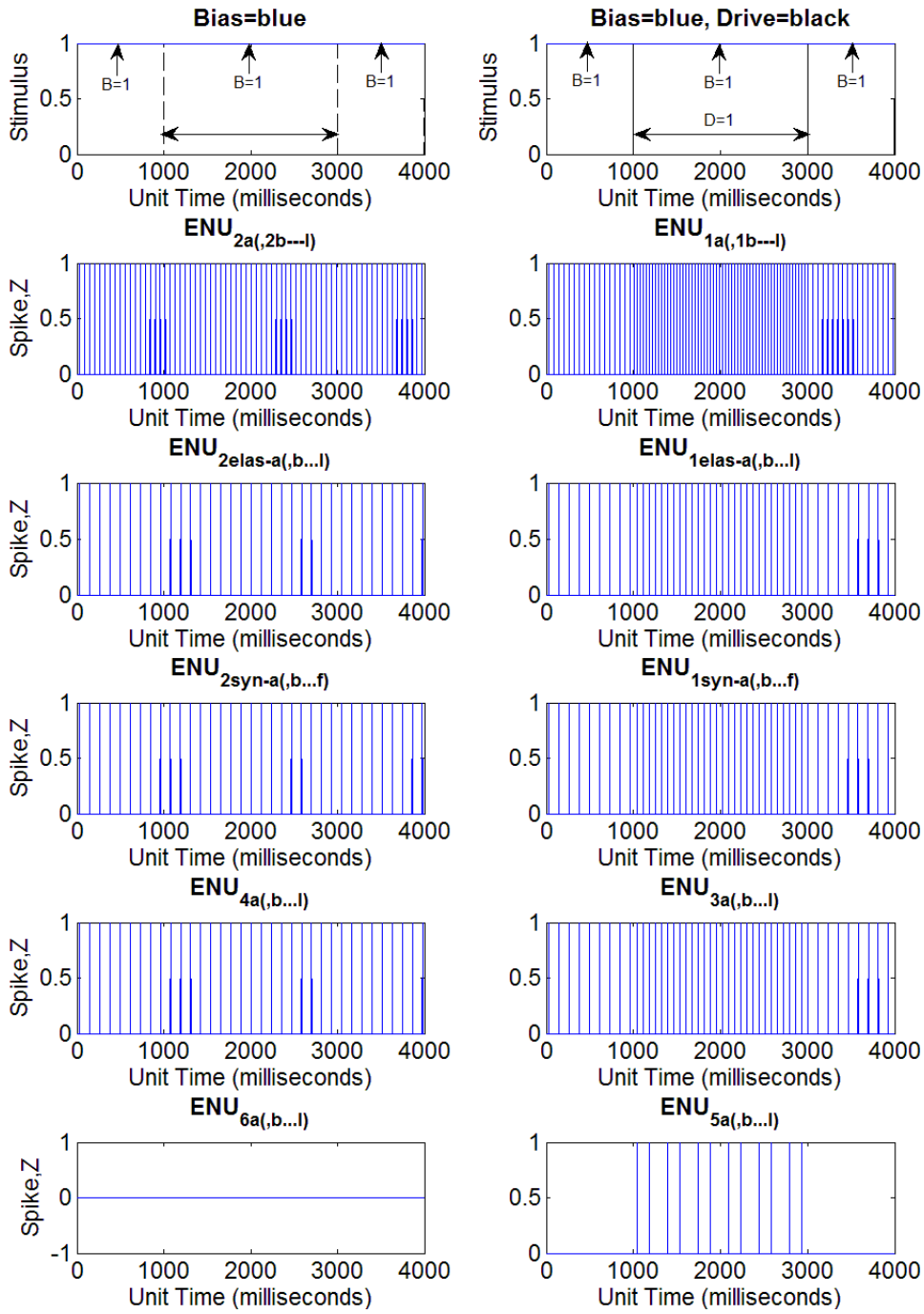

Figure 3.23. Output traces of one basic ENU (ENU_{xa}) implemented (out of 12 each in ENU_1 & ENU_2, 6 each in ENU_{1syn} & ENU_{2syn}, 12 each in ENU_{1elas} & ENU_{2elas}, 12 each in ENU_3 & ENU_4 and 12 each in ENU_5 & ENU_6 group) in E-DN architecture of Figure 3.21 receiving both B and D-stimulus using same parameters (table 3.5).

This outcome for the current E-DN (Fig. 3.23) shows slowing of spiking rates in ENU groups (ENU_{1elas} & ENU_{1syn} also ENU_{2elas} & ENU_{2syn}) within the first two nodes (Eck1 & Eck2) which do not receive the B or D-stimulus directly. During just B-stimulus equally strong inputs from Eck3 and Eck4 cancel each other out resulting in desired output traces (G-DN property) of Eck5 and Eck6. However the netlet within first two nodes might still be modified such that it is effective only during dual-stimuli (during B & D) thus retaining the achieved G-DN property but altering the amount of spiking during dual stimuli (causing elastic property). This was studied next.

Four ENU groups within initial nodes (node-1 or Eck1 & node-2 or Eck2)

The E-DN architecture in Figure 3.21 was modified based on the intuition that the network behavior may differ from Figure 3.23 if there is a decrease in inhibition from ENU_{1elas} to ENU_{1syn} (ENU groups in nodes receiving the additional D-stimulus) during dual-stimuli. That is, the additional D-stimulus during dual-stimuli causes decreased output from ENU_{1elas} group. Therefore, during just B-stimulus there are no outputs from the network ends (Eck5 & Eck6) due to the equally active initial nodes (Eck1 & Eck3 for Eck5 and Eck2 & Eck4 for Eck6). But during dual-stimuli Eck3 has more activity relative to Eck4 causing inhibition Eck6 but excitation of Eck5.

For reduced inhibition of ENU_{1syn} only during dual stimuli another ENU group (ENU_{1modu} & ENU_{2modu}) is added in the first two nodes (Eck1 & Eck2 respectively) such that they respond/spike only during dual-stimuli as shown in Figures 3.24 and 3.25. To observe the behavior of this E-DN, simulation was done using parameters given in table 3.6. Results are shown in Figure 3.26.

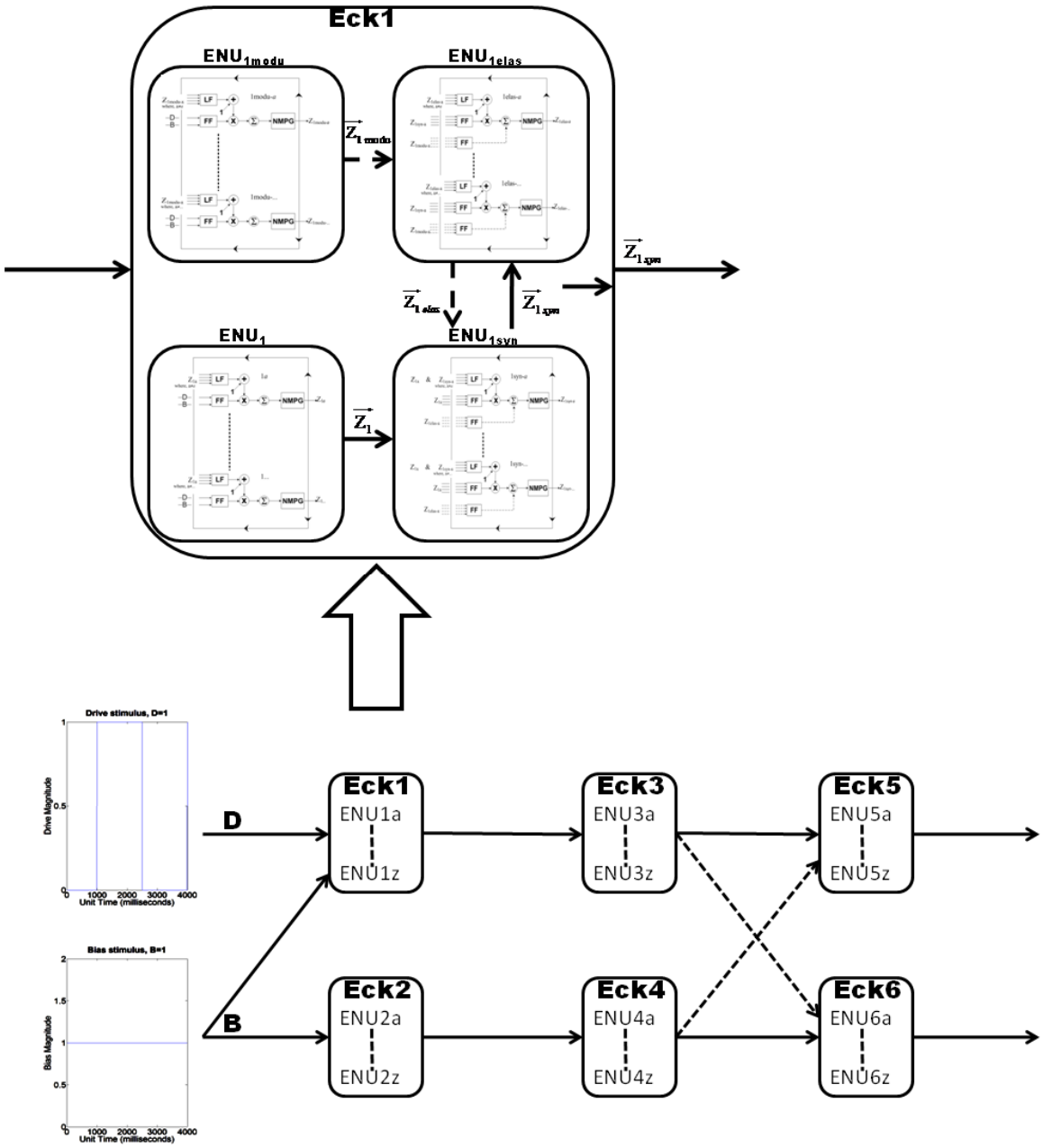

Figure 3.24. E-DN with four ENU groups (ENU_1, ENU_{1syn}, ENU_{1elas} & ENU_{1modu}) in Eck1 (and Eck2) such that ENU_{1elas} receives inhibitory pulsed inputs from ENU_{1modu} and also excitatory inputs from ENU_{1syn}. Number of basic ENU's per ENU groups: 12 each in ENU_1 & ENU_2, 6 each in ENU_{1syn} & ENU_{2syn}, , 12 each in ENU_{1modu} & ENU_{2modu}, 12 each in ENU_{1elas} & ENU_{2elas}; 12 each in ENU_3 & ENU_4 and 12 each in ENU_5 & ENU_6.

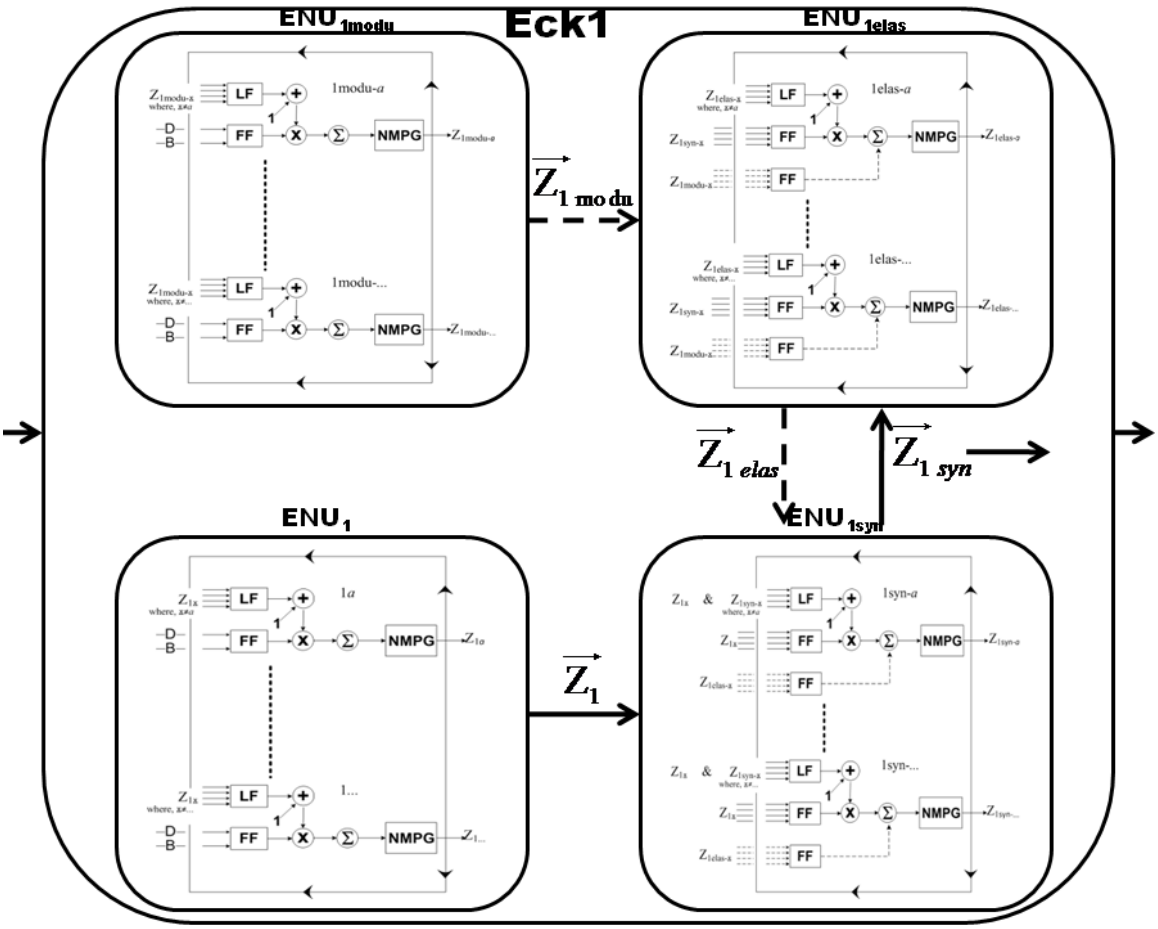

Figure 3.25. Enlarged view of the inset seen in Figure 3.24 showing the configuration of *n*-basic ENU's amongst the four ENU groups (ENU_1, ENU_{1syn}, ENU_{1elas} & ENU_{1modu}) within Eck1.

Feeding field (FF) for all basic ENU's within ENU_1 and ENU_{1modu} group receives input stimulus which in the case of node-1 (Eck1) is the drive (D) and bias (B) stimulus as DC. Outputs of ENU_1 group ($\vec{Z}_1$) are the inputs for the FF of basic ENU's within ENU_{1syn} group. However, outputs of ENU_{1modu} group ($\vec{Z}_{1modu}$) are the inputs for the inhibitory dendrite FF of basic ENU's within ENU_{1elas} group.

ENU_{1syn} group outputs ($\vec{Z}_{1syn}$) in turn are the inputs for the excitatory dendrite FF of basic ENU's within ENU_{1elas} group. The ENU_{1elas} outputs ($\vec{Z}_{1elas}$) are then inputs for the FF of inhibitory dendrite of ENU_{1syn} (i.e., lateral inhibition).

Finally, inputs for Eck3 and Eck4 are from ENU_{1syn} ($\vec{Z}_{1syn}$) of Eck1 and ENU_{2syn} ($\vec{Z}_{2syn}$) of Eck2 respectively.

		E-DN Node								
		1 or 2						3 or 4	5 or 6	
		ENU Group								
ENU Part		ENU_1 or ENU_2	ENU_{1modu} or ENU_{2modu}	ENU_{1syn} or ENU_{2syn}		ENU_{1elas} or ENU_{2elas}		ENU_3 or ENU_4	ENU_5 or ENU_6	
		Basic ENU								
Dend.		$ENU_{1a(b,\ldots,l)}$ or $ENU_{2a(b,\ldots,l)}$	$ENU_{1modu\text{-}a(b,\ldots,l)}$ or $ENU_{2modu\text{-}a(b,\ldots,l)}$	$ENU_{1syn\text{-}a(b,\ldots,f)}$ or $ENU_{2syn\text{-}a(b,\ldots,f)}$		$ENU_{1elas\text{-}a(b,\ldots,l)}$ or $ENU_{2elas\text{-}a(b,\ldots,l)}$		$ENU_{3a(b,\ldots,l)}$ or $ENU_{4a(b,\ldots,l)}$	$ENU_{5a(b,\ldots,l)}$ or $ENU_{6a(b,\ldots,l)}$	
LF	w_{lf}	0.5	-	0.5		5		0.5	0.5	
	τ_{lf}	1	-	1		1		1	1	
FF	w_{ff}	0.5	0.25	$1^{(+)}$	$125^{(-)}$	$1^{(+)}$	$0.5^{(-)}$	1	$0.5^{(+)}$	$2^{(-)}$
	τ_{ff}	10	20	$10^{(+)}$	$30^{(-)}$	$10^{(+)}$	$30^{(-)}$	10	$10^{(+)}$	$40^{(-)}$

Table 3.6. Parameters used for the simulation (Fig. 3.26) of E-DN architecture shown in Figure 3.24. Note the lack of linking field in ENU's within ENU_{1modu} & ENU_{2modu} groups. The parameters for soma/neuromime remain the same as in table 3.1.

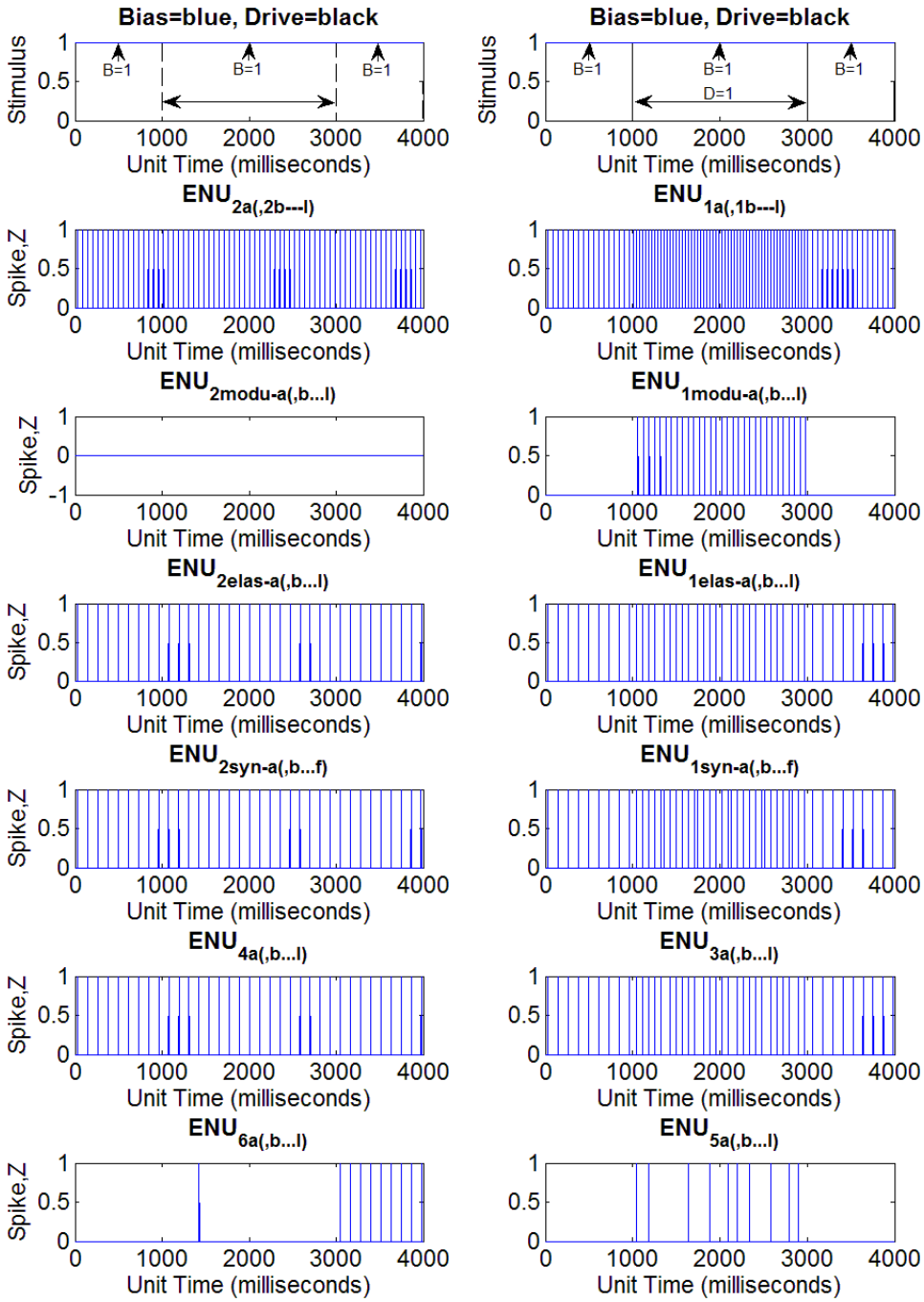

Figure 3.26. Output traces of one basic ENU (ENU_{xa}) implemented (out of 12 each in ENU_1 & ENU_2, 12 each in ENU_{1modu} & ENU_{2modu}, 6 each in ENU_{1syn} & ENU_{2syn}, 12 each in ENU_{1elas} & ENU_{2elas}, 12 each in ENU_3 & ENU_4 and 12 each in ENU_5 & ENU_6 group) in E-DN architecture of Figure 3.24 receiving both B and D-stimulus using parameters (table 3.6).

Output (Fig. 3.26) from Eck5 and Eck6 shows that addition of ENU group (ENU_{1mod} & ENU_{2mod}) responding only during dual-stimuli has altered the spikes. During dual-stimuli and B-stimulus preceding it, Eck5 and Eck6 response is similar to the previous E-DN (Fig. 3.23). However, after removal of D-stimulus spikes occur in Eck6. But this is not the elastic property since it continuously spikes, never getting inhibited from the equally strong pulsed inputs of Eck3.

Five ENU groups within initial nodes (node-1 or Eck1 & node-2 or Eck2)

An alternate connection to the present E-DN (Fig. 3.24 & 3.26) is for ENU_{1elas} and ENU_{2elas} groups to receive excitatory inputs in place of inhibition from ENU_{1mod} and ENU_{2mod} respectively. This would result in ENU_{1syn} group receiving increased inhibition during dual-stimuli. But inhibition by ENU_{1mod} group during dual-stimuli successfully altered the spiking from succeeding nodes (Fig. 3.26). This can be done by decreasing/ weakening the inhibition of ENU_{1syn} and ENU_{2syn} (from respective ENU_{1elas} and ENU_{2elas}) during just B-stimulus to counterbalance the increased inhibition during dual-stimuli.

To achieve the above described network another ENU group is added to the first two nodes (Eck1 & Eck2). The reason is that excitation of ENU_{1elas} group only during dual-stimuli will be from ENU_{1mod}, which is responsive only during this condition while all other ENU groups within Eck1 and Eck2 spike irrespective of this. Thus for weakening the inhibition of ENU_{1syn} and ENU_{2syn}, i.e., inhibiting ENU_{1elas} and ENU_{2elas} (during B stimulus) another ENU group is added in Eck1 ($ENU_{1m\text{-}elas}$) and Eck2 ($ENU_{2m\text{-}elas}$). Thus $ENU_{1m\text{-}elas}$ and $ENU_{2m\text{-}elas}$ outputs occur only during B-stimulus. The new E-DN is shown

in Figures 3.27 and 3.28. Simulation of this network (Fig. 3.29) was done with the parameters given in table 3.7.

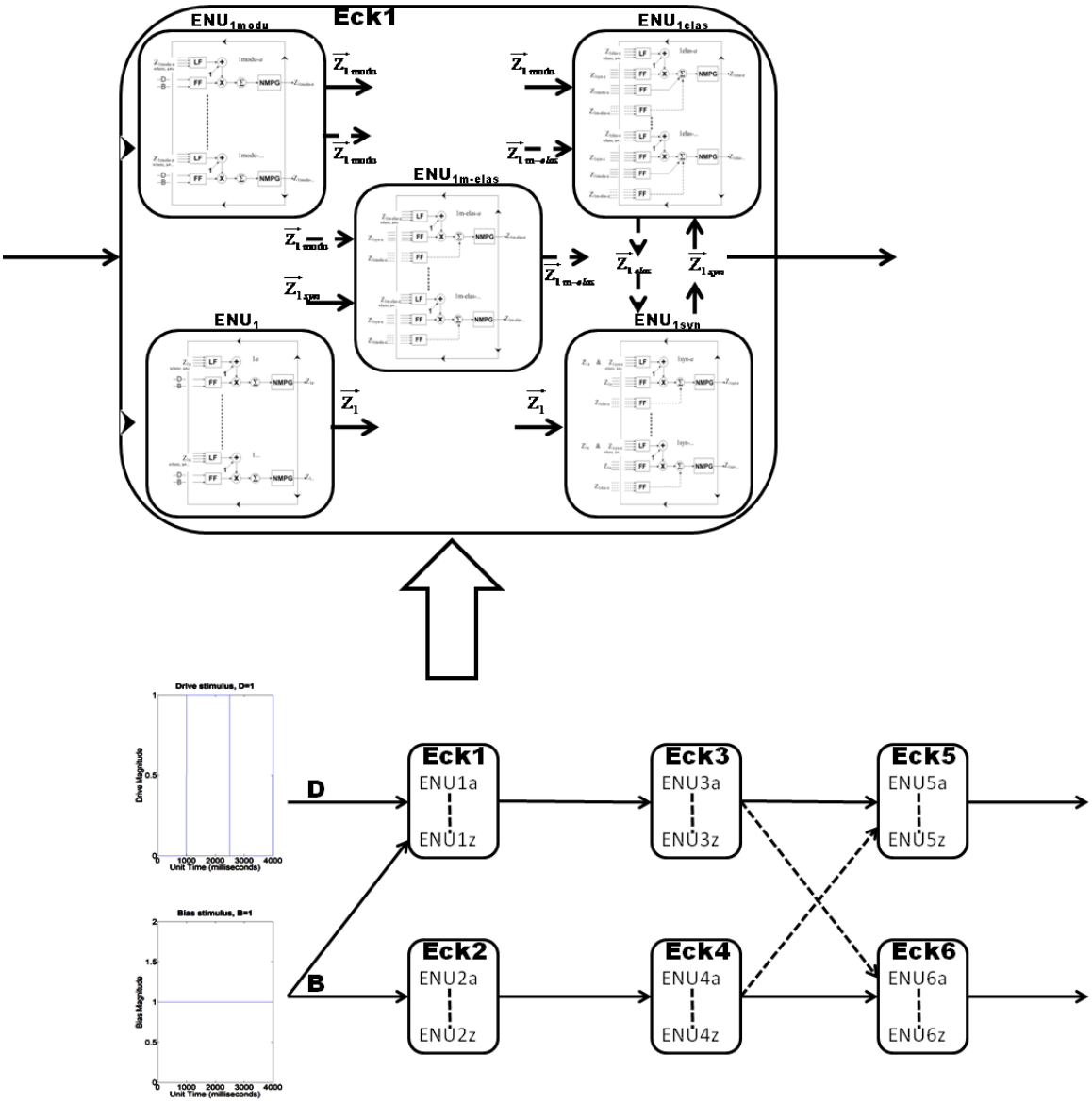

Figure 3.27. E-DN with five ENU groups (ENU_1, ENU_{1syn}, ENU_{1elas}, ENU_{1modu} & $ENU_{1m\text{-}elas}$) in Eck1 (and Eck2) such that ENU_{1elas} receives excitatory pulsed inputs from ENU_{1modu} & ENU_{1syn} but receives inhibitory inputs from $ENU_{1m\text{-}elas}$. The $ENU_{1m\text{-}elas}$ receives excitatory inputs from ENU_{1syn} but inhibitory from ENU_{1modu}.Number of basic ENU's per ENU groups: 12 each in ENU_1 & ENU_2, 6 each in ENU_{1syn} & ENU_{2syn}, 12 each in ENU_{1modu} & ENU_{2modu}, 12 each in ENU_{1elas} & ENU_{2elas}, 12 each in $ENU_{1m\text{-}elas}$ & $ENU_{2m\text{-}elas}$, 12 each in ENU_3 & ENU_4 and 12 each in ENU_5 & ENU_6.

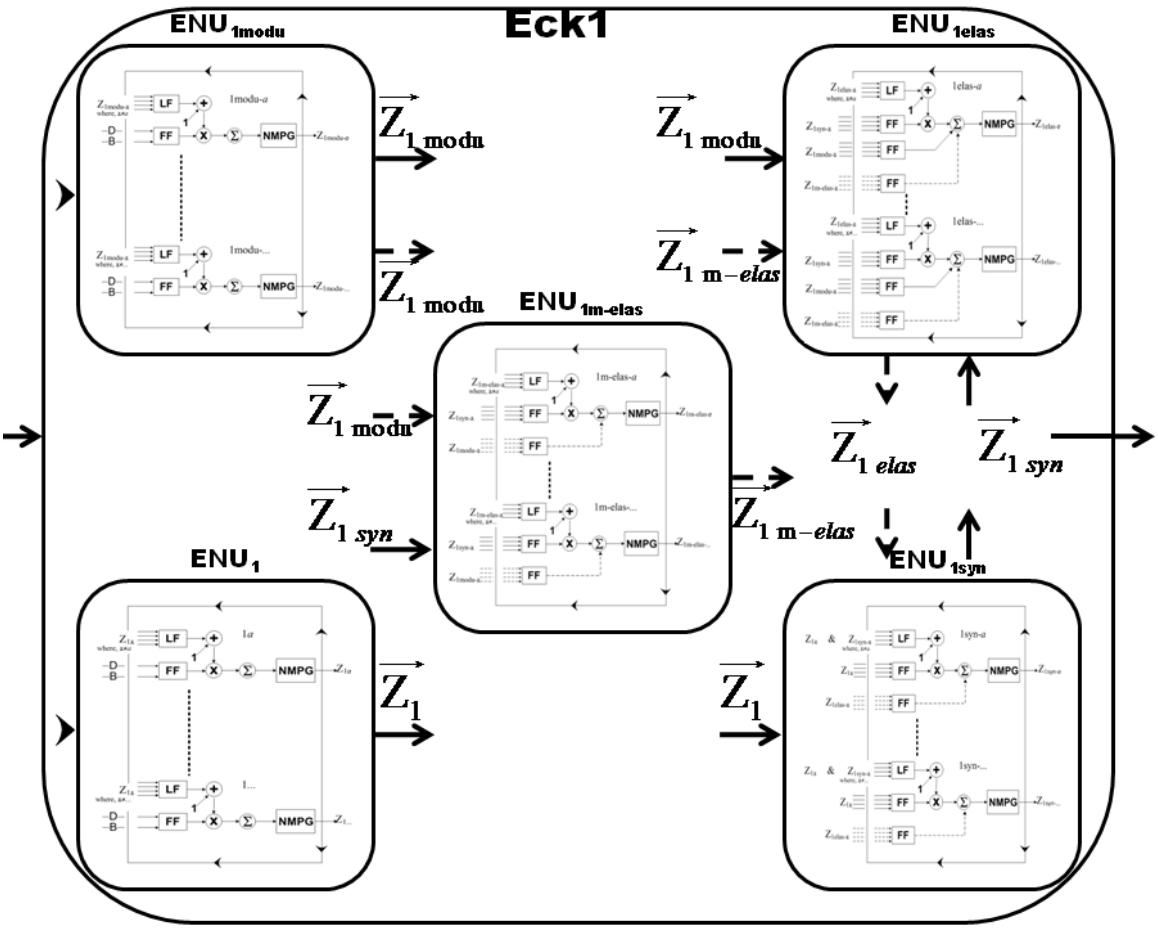

Figure 3.28. Enlarged view of the inset seen in Figure 3.27 showing the configuration of n basic ENU's amongst the five ENU groups (ENU_1, ENU_{1syn}, ENU_{1elas}, ENU_{1modu} & $ENU_{1m\text{-}elas}$) within Eck1.

Feeding field (FF) for all basic ENU's within ENU_1 and ENU_{1modu} group receives input stimulus, which in the case of Eck1 is the drive (D) and bias (B) stimulus as DC. Outputs of ENU_1 group ($\vec{Z}_1$) are the inputs for the excitatory dendrite FF of basic ENU's within ENU_{1syn} group. However, outputs of ENU_{1modu} group ($\vec{Z}_{1modu}$) are the inputs for the excitatory dendrite FF of basic ENU's within ENU_{1elas} group but inputs for inhibitory dendrite FF of basic ENU's within $ENU_{1m\text{-}elas}$ group.

ENU_{1syn} group outputs ($\vec{Z}_{1syn}$) in turn are the inputs for another excitatory dendrite FF of basic ENU's within ENU_{1elas} group and also inputs for excitatory dendrite FF of basic ENU's within $ENU_{1m\text{-}elas}$ group. The $ENU_{1m\text{-}elas}$ outputs ($\vec{Z}_{1m-elas}$) are then inputs for the FF of inhibitory dendrite of ENU_{1elas}.

Finally, ENU_{1elas} outputs ($\vec{Z}_{1elas}$) are the inputs for the FF of inhibitory dendrite of ENU_{1syn} (i.e., lateral inhibition). And inputs for Eck3 and Eck4 are from ENU_{1syn} ($\vec{Z}_{1syn}$) of Eck1 and ENU_{2syn} ($\vec{Z}_{2syn}$) of Eck2 respectively.

		E-DN Node										
		1 or 2								3 or 4	5 or 6	
		ENU Group										
ENU Part		ENU_1 or ENU_2	ENU_{1modu} or ENU_{2modu}	ENU_{1syn} or ENU_{2syn}		ENU_{1elas} or ENU_{2elas}		$ENU_{1m\text{-}elas}$ or $ENU_{2m\text{-}elas}$		ENU_3 or ENU_4	ENU_5 or ENU_6	
		Basic ENU										
Dend.		$ENU_{1a(b,\ldots,l)}$ or $ENU_{2a(b,\ldots,l)}$	$ENU_{1modu\text{-}a(b,\ldots,l)}$ or $ENU_{2modu\text{-}a(b,\ldots,l)}$	$ENU_{1syn\text{-}a(b,\ldots,l)}$ or $ENU_{2syn\text{-}a(b,\ldots,l)}$		$ENU_{1elas\text{-}a(b,\ldots,l)}$ or $ENU_{2elas\text{-}a(b,\ldots,l)}$		$ENU_{1m\text{-}elas\text{-}a(b,\ldots,l)}$ or $ENU_{2m\text{-}elas\text{-}a(b,\ldots,l)}$		$ENU_{3a(b,\ldots,l)}$ or $ENU_{4a(b,\ldots,l)}$	$ENU_{5a(b,\ldots,l)}$ or $ENU_{6a(b,\ldots,l)}$	
LF	w_{lf}	0.5	0.25	0.5		5		0.5		0.5	0.5	
	τ_{lf}	1	1	1		1		1		1	1	
FF	w_{ff}	5	0.25	$1^{(+)}$	$125^{(-)}$	$1^{(+)}$ $0.35^{(+)}$	$1^{(-)}$	$1^{(+)}$	$5^{(-)}$	1	$0.5^{(+)}$	$2^{(-)}$
	τ_{ff}	10	15	$10^{(+)}$	$30^{(-)}$	$10^{(+)}$	$30^{(-)}$	$10^{(+)}$	$40^{(-)}$	10	$10^{(+)}$	$40^{(-)}$

Table 3.7. Parameters used for simulation (Fig. 3.29) of E-DN architecture shown in Figure 3.27. Note: (+) input w_{ff} for ENU_{1elaas} & ENU_{2elas} are different; w_{ff}=1 from ENU_{1syn} & w_{ff}=0.35 from ENU_{1modu}. The parameters for soma/neuromime remain same as in table 3.1.

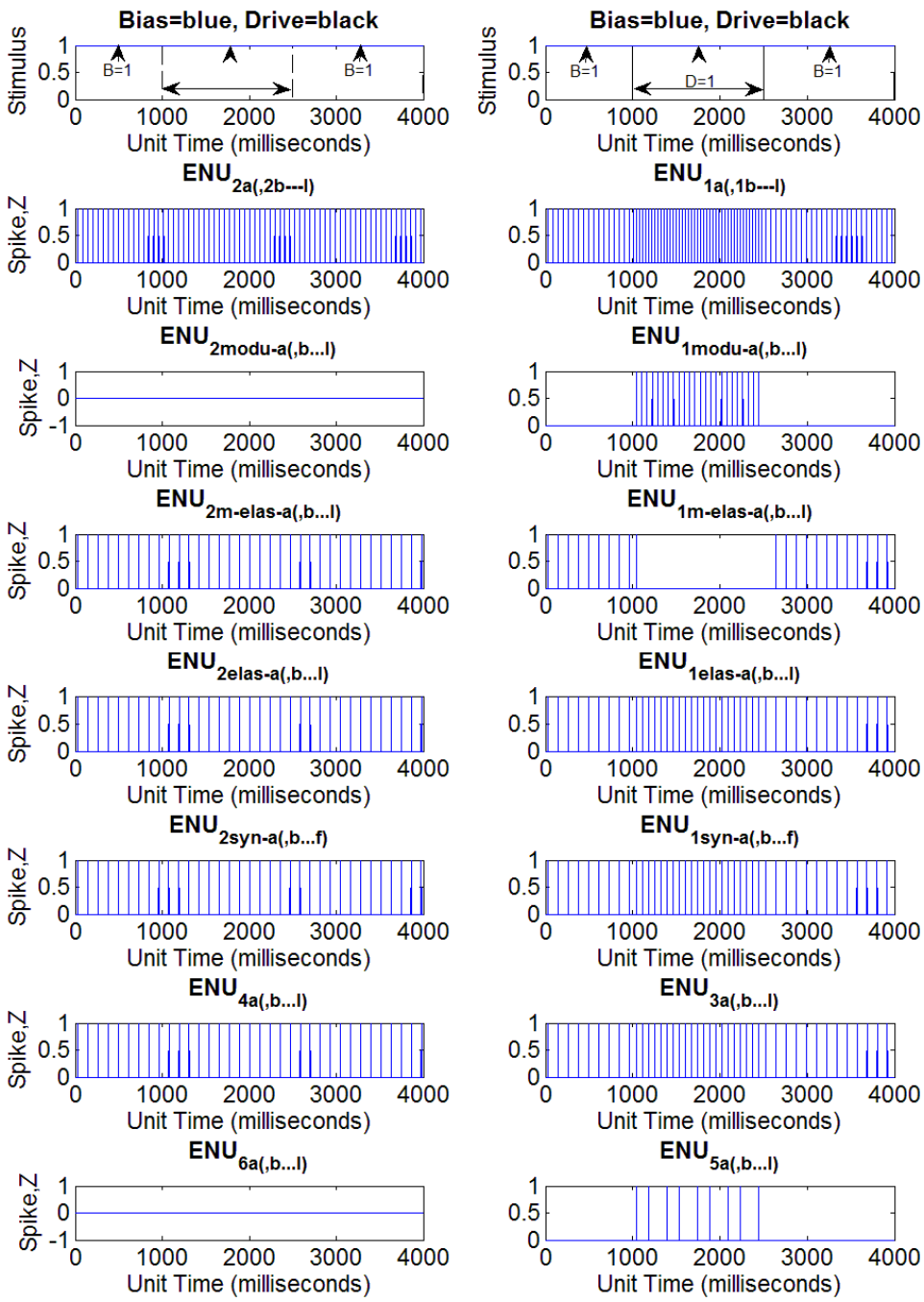

Figure 3.29. Output traces of one basic ENU (ENU_{xa}) implemented (out of 12 each in ENU_1 & ENU_2, 12 each in ENU_{1modu} & ENU_{2modu}, 6 each in ENU_{1syn} & ENU_{2syn}, 12 each in ENU_{1elas} & ENU_{2elas}, 12 each in $ENU_{1m\text{-}elas}$ & $ENU_{2m\text{-}elas}$, 12 each in ENU_3 & ENU_4 and 12 each in ENU_5 & ENU_6 group) in E-DN architecture of Figure 3.27 receiving both B and D-stimulus using parameters in table 3.7.

Outcome of the simulation (Fig. 3.29) resembles the outputs seen earlier (Fig. 3.23) for the E-DN shown in Figure 3.21. This output traces implies increased inhibition of ENU_{1syn} during dual-stimuli. But during B-stimulus the inhibition of ENU_{1elas} and ENU_{2elas} may be insufficient, causing these ENU groups to continue inhibiting ENU_{1syn} and ENU_{2syn} respectively. This is most probably linked with the excessively strong inhibitory feeding field weight ($w_{ff} = 125^{(-)}$) for ENU_{1syn} and ENU_{2syn} (table 3.7). The strong inhibitory feeding field weight parameter has been used since the introduction of ENU_{1elas} and ENU_{2elas} group (Fig. 3.21) with the intent to set a plausible value after achieving the desired network during the build-up process.

Since the introduction of ENU_{1syn} and ENU_{2syn} groups in Eck1 and Eck2 respectively (Fig. 3.17), all pulsed inputs for Eck3 and Eck4 have been from respective ENU_{1syn} and ENU_{2syn} groups. This was also the case in the current E-DN (Fig. 3.27). A different alternative for outputs from first two nodes (Eck1 & Eck2) may be attempted due to failures with networks yet designed.

Inputs for node-3 (Eck3) and node-4 (Eck4) from different ENU groups within the first two nodes (Eck1 & Eck2)

Eck3 and Eck4 inputs from outputs of ENU_1 and ENU_{1syn} (also ENU_2 & ENU_{2syn}) groups within Eck1 might not be the best choice since the main purpose of adding ENU_{1syn} (and ENU_{2syn}) was to achieve synchronization. The output traces (Fig. 3.29) of ENU_{1elas} (and ENU_{2elas}) appear to be similar to ENU_{1syn} (and ENU_{2syn}) and hence will likely produce a similar outcome as Figure 3.29 if outputs from ENU_{1elas} (and ENU_{2elas}) are chosen as inputs for Eck3 (and Eck4). Thus suitable ENU groups can be narrowed

down to a combination of ENU_{1mod} and $ENU_{1m\text{-}elas}$ (also ENU_{2mod} & $ENU_{2m\text{-}elas}$) since during just B-stimulus, outputs from first two nodes (Eck1 & Eck2) would be same due to $ENU_{1m\text{-}elas}$ (and $ENU_{2m\text{-}elas}$) but during dual-stimuli ENU_{1mod} receiving the additional D-stimulus, would be capable of causing spiking in Eck5.

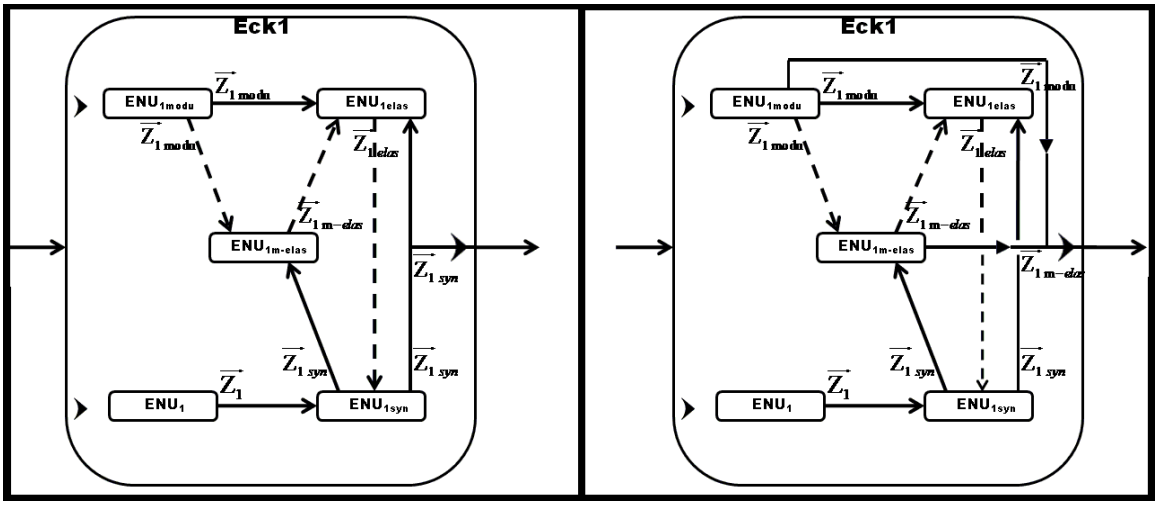

Figure 3.30. Two output configuration for Eck1 (similarly for Eck2, not shown).

Left shows the configuration used for simulating the output traces of figure 3.29 where ENU_{1syn} is the source of pulsed outputs from Eck1 (and similarly ENU_{2syn} for Eck2).

Right shows the new configuration such that both ENU_{1modu} and $ENU_{1m\text{-}elas}$ are the source of output. Both outputs are excitatory (solid line).

Though the figure (right) shows two lines joining to give a single arrow out of Eck1, outputs from the two ENU groups do not summate. However the input vector for Eck3 feeding field has elements of the two ENU group outputs ($\vec{Z}_{1modu}$ & $\vec{Z}_{1m-elas}$).

With the new output configuration shown in Figure 3.30 (right) implemented for first two nodes (Eck1 & Eck2) and everything else remaining the same (Fig. 3.27), the new E-DN is derived. The new E-DN was then simulated (Fig. 3.31) with the same parameters (table 3.7) used for previous network.

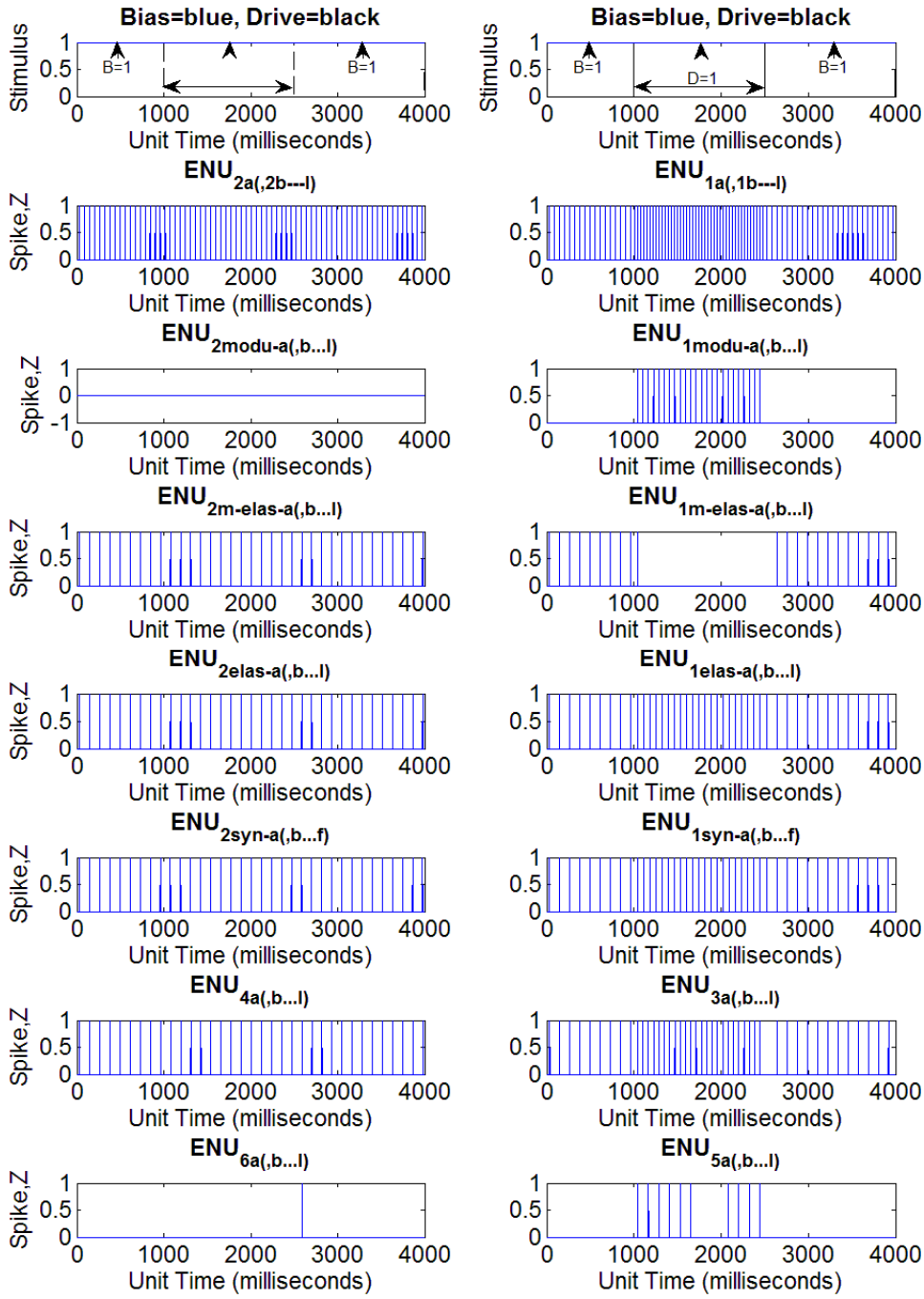

Figure 3.31. Output traces of one basic ENU (ENU_{xa}) implemented (out of 12 each in ENU_1 & ENU_2, 12 each in ENU_{1modu} & ENU_{2modu}, 6 each in ENU_{1syn} & ENU_{2syn}, 12 each in ENU_{1elas} & ENU_{2elas}, 12 each in $ENU_{1m\text{-}elas}$ & $ENU_{2m\text{-}elas}$, 12 each in ENU_3 & ENU_4 and 12 each in ENU_5 & ENU_6 group) in E-DN architecture similar to Figure 3.27 but with output configuration of first two node given by Figure 3.30 (right) receiving both B and D-stimulus using parameters in table 3.7.

The simulation result (Fig. 3.31) shows output in Eck6 soon after the removal of D-stimulus before the equally strong excitatory and inhibitory inputs prevent further outputs from Eck5 and Eck6. This shows that the network, in addition to replicating the property of G-DN encountered in Figure 3.23, also has the potential for replicating the elastic property. The observed results however cannot be considered elastic property since to correspond to the activity seen in G-DN (Fig. 3.7), even though the G-DN activity is very small, Eck6 output should be more than one spike to maintain consistency in activity equivalence mapping between G-DN and E-DN (transformed spikes, Chapter-2, p36-37).

At this stage of network design, with certain amount of success achieved, it was appropriate to refine the E-DN. It should also be mentioned here that the current E-DN has two major problems; some parameter values and the number of basic ENU's implemented. Amongst the parameter values used, the inhibitory feeding field weight ($w_{ff} = 125^{(-)}$) for ENU_{1syn} and ENU_{2syn} is very large (table 3.7). This excessively large w_{ff} for ENU_{1syn} and ENU_{2syn} implies strong inhibition from ENU_{1elas} and ENU_{2elas} respectively. This could be interpreted as, E-DN having many more basic ENU's within ENU_{1elas} and ENU_{2elas} groups (more than 20 each). Hence the two issues are interlinked.

Removal of redundant ENU's and ENU groups

The number of usages of basic ENU's is important not only in terms of computability or computing time but also for making any plausible physical or biological meaning. Basic ENU's are not models at the neuronal level but, due to the absence of reset function, they are abstract model at population level [Wells 2010, Ch.8]. The number of basic ENU's in just the first node (Eck1) of current E-DN is 54 with a total of 166 in all

the six nodes. Considering basic ENU's as population of neurons, usage of such an amount of neuronal resource seems not only unlikely but disadvantageous in the physical world because dipole networks perform a small function in the grand scheme of nervous system.

Refining the current network would therefore mean pruning or removing any redundant ENU groups or basic ENU's within ENU groups. In the current network (Fig. 3.27 but with Eck1 & Eck2 output as shown in Fig. 3.30 right) the purpose of the ENU_{1syn} and ENU_{1elas} groups is eventually to stimulate $ENU_{1m\text{-}elas}$ (similarly for Eck2). Thus only three ENU groups could be implements in the Eck1; ENU_1, ENU_{1modu} and $ENU_{1m\text{-}elas}$ (and similarly for Eck2). This also means that the issue of excessively strong inhibitory feeding field weight ($w_{ff} = 125^{(-)}$) will not exist since ENU_{1syn} (and ENU_{2syn}) is no longer a component of Eck1 (and Eck2). The transformation from 5 ENU groups each per Eck1 and Eck2 to 3 ENU groups is shown in Figures 3.32 through 3.34.

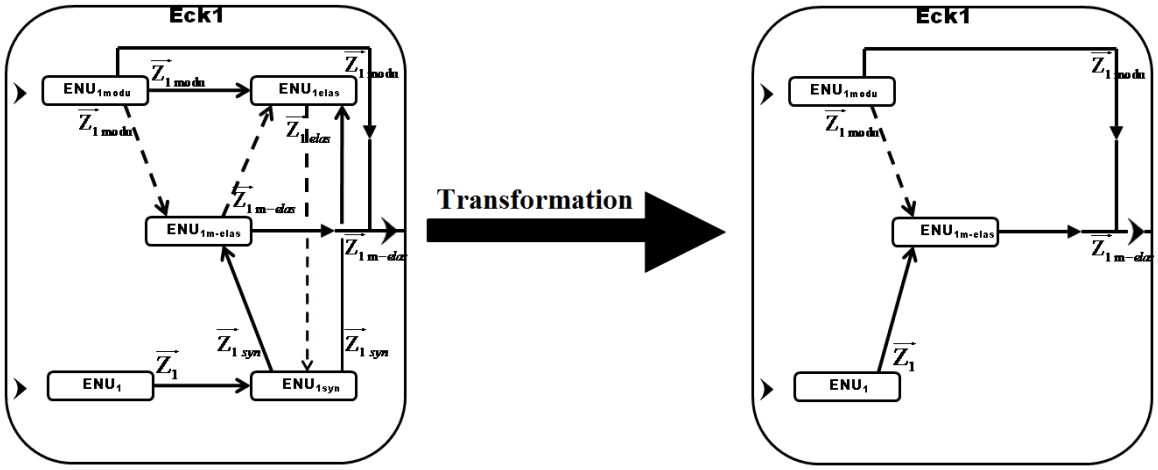

Figure 3.32. Transformation of the components within Eck1 of E-DN following removal of redundant ENU groups (ENU_{1syn} & ENU_{1elas}). Note that though the two ENU groups have been pruned, considering them as redundant, $ENU_{1m\text{-}elas}$ still needs to receive stimulus for it to respond correspondingly to the input (B & D). This is done by receiving excitatory pulsed inputs from ENU_1.

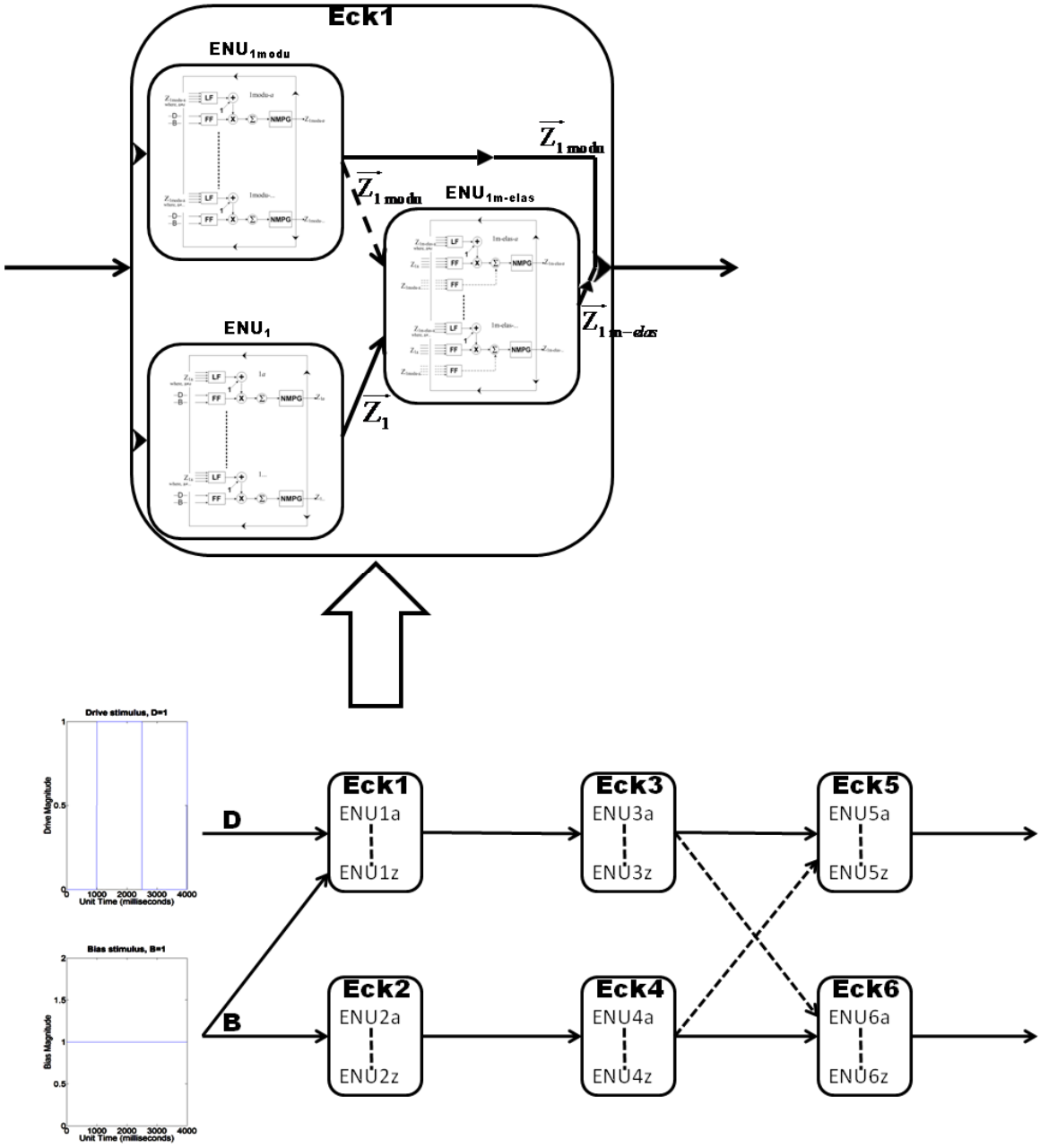

Figure 3.33. E-DN with three ENU groups (ENU_1, ENU_{1modu} & $ENU_{1m\text{-}elas}$) in Eck1 (and Eck2) such that $ENU_{1m\text{-}elas}$ receives excitatory pulsed inputs from ENU_1 but receives inhibitory inputs from ENU_{1modu}. Then both $ENU_{1m\text{-}elas}$ & ENU_{1modu} send outputs for Eck1. Number of basic ENU's per ENU groups: 5 each in ENU_1 & ENU_2, 5 each in ENU_{1modu} & ENU_{2modu}, 5 each in $ENU_{1m\text{-}elas}$ & $ENU_{2m\text{-}elas}$, 2 each in ENU_3 & ENU_4 and 2 each in ENU_5 & ENU_6.

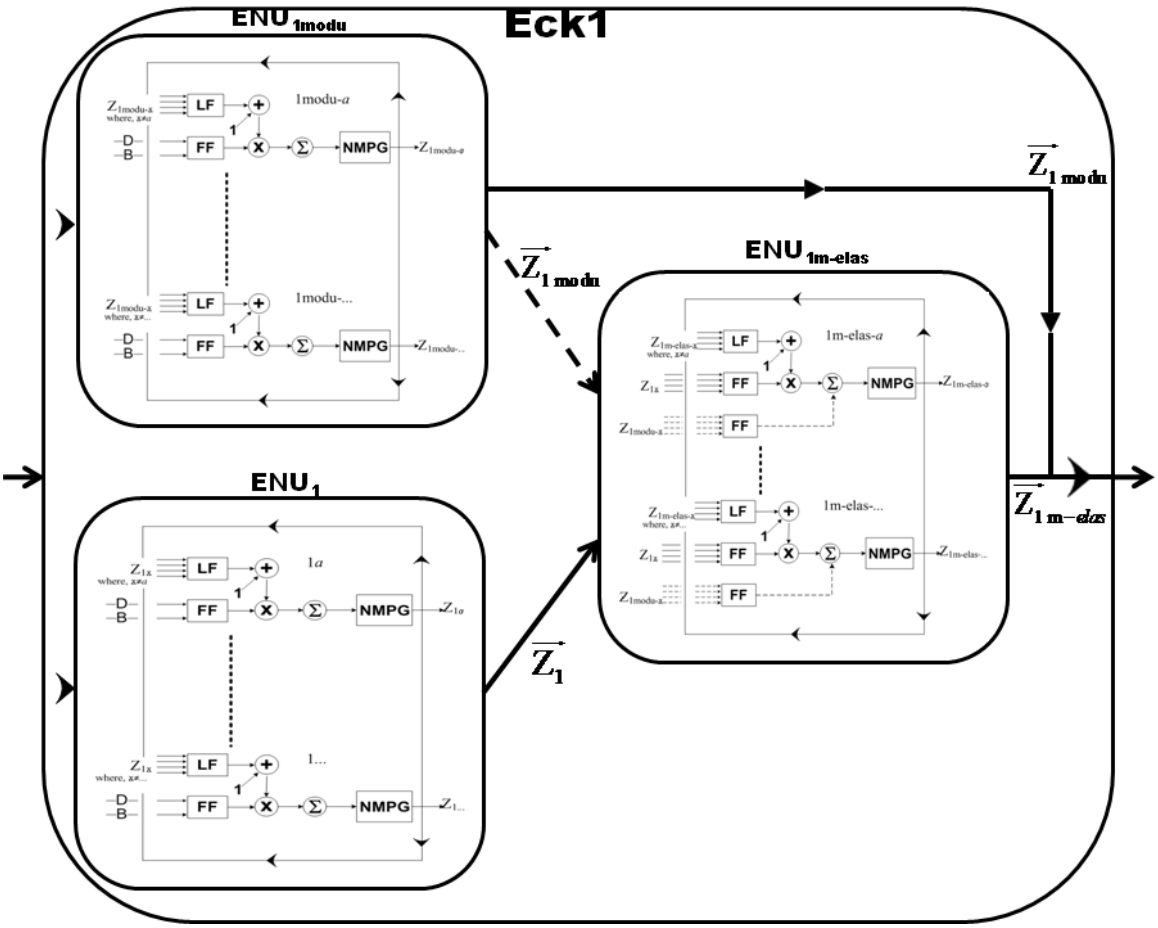

Figure 3.34. Enlarged view of the inset seen in Figure 3.33 showing the configuration of n basic ENU's amongst the three ENU groups (ENU_1, ENU_{1modu} & $ENU_{1m\text{-}elas}$) within Eck1.

Feeding field (FF) for all basic ENU's within ENU_1 and ENU_{1modu} group receives input stimulus which in the case of Eck1 is the drive (D) and bias (B) stimulus as DC. Outputs of ENU_1 group ($\vec{Z}_1$) are the inputs for the excitatory dendrite FF of basic ENU's within $ENU_{1m\text{-}elas}$ group. However, outputs of ENU_{1modu} group ($\vec{Z}_{1modu}$) are the inputs for the inhibitory dendrite FF of basic ENU's within $ENU_{1m\text{-}elas}$ group.

Finally, inputs for Eck3 and Eck4 are from ENU_{1modu} ($\vec{Z}_{1modu}$) and $ENU_{1m\text{-}elas}$ ($\vec{Z}_{1m-elas}$) of Eck1 and from ENU_{2modu} ($\vec{Z}_{2modu}$) and $ENU_{2m\text{-}elas}$ ($\vec{Z}_{2m-elas}$) of Eck2 respectively.

Further pruning of the network can be done by decreasing the number of basic ENU's in other nodes apart from the first two nodes (Eck1 & Eck2) as shown in Figure 3.34 and 3.35. It should be noted that the new E-DN has 15 basic ENU's in Eck1 and a total of 38,

which is considerably less than 54 and 166 total for the previous network. New parameter values (table 3.8) were then used for simulation of the new E-DN. The result is shown in Figure 3.36.

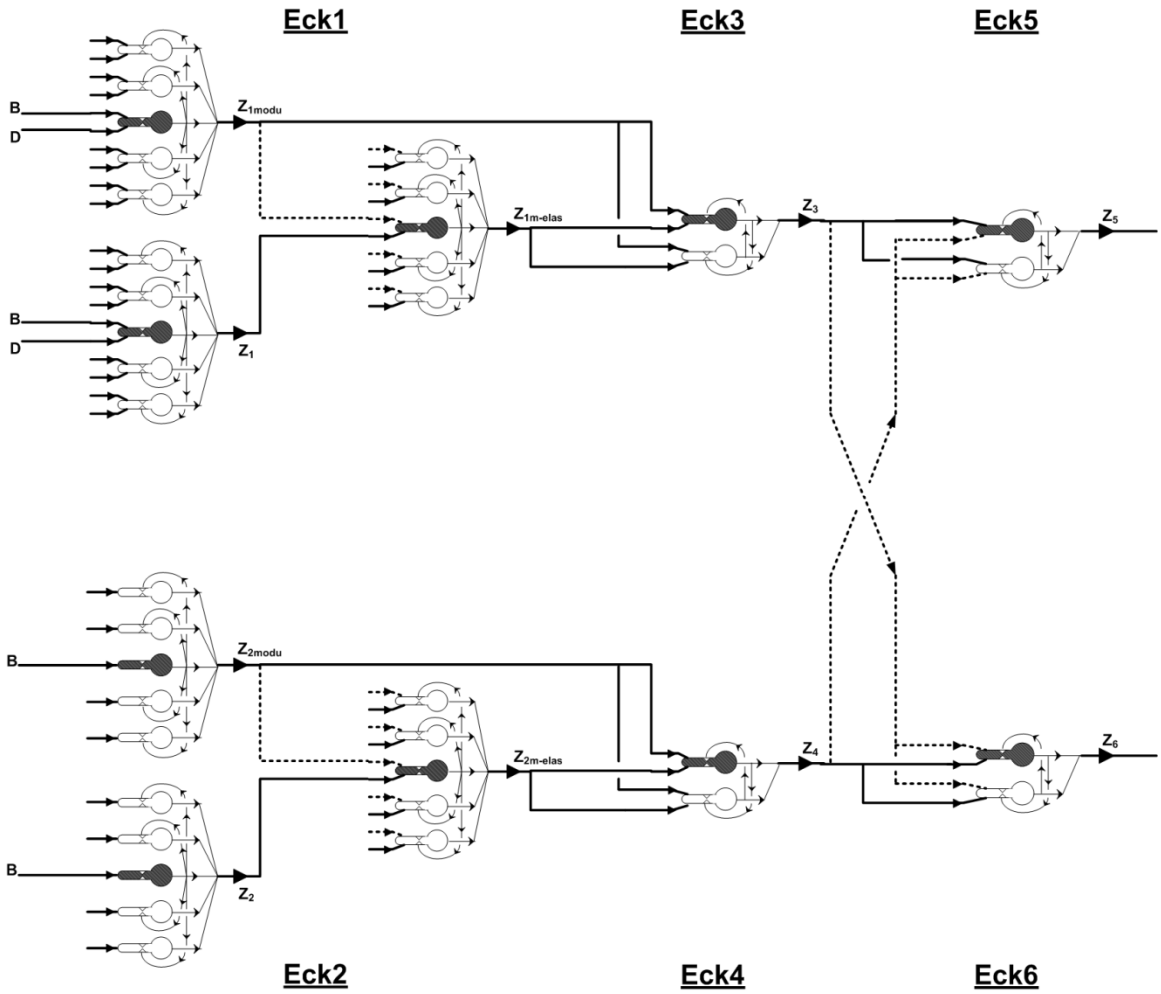

Figure 3.35. Dipole Network using basic ENU as seen in Figure 2.5. Connections of one basic ENU per ENU group in the nodes (shaded basic ENU's) is shown for clarity. Notation for the lines representing connection are same as before (solid for excitatory and dashed for inhibitory).

ENU Part Dend.		E-DN Node						
		1 or 2				3 or 4	5 or 6	
		ENU Group						
		ENU_1 or ENU_2	ENU_{1modu} or ENU_{2modu}	$ENU_{1m\text{-}elas}$ or $ENU_{2m\text{-}elas}$		ENU_3 or ENU_4	ENU_5 or ENU_6	
		Basic ENU						
		$ENU_{1a(b,\ldots,e)}$ or $ENU_{2a(b,\ldots,e)}$	$ENU_{1modu\text{-}a(b,\ldots,e)}$ or $ENU_{2modu\text{-}a(b,\ldots,e)}$	$ENU_{1m\text{-}elas\text{-}a(b,\ldots,e)}$ or $ENU_{2m\text{-}elas\text{-}a(b,\ldots,e)}$		$ENU_{3a(3b)}$ or $ENU_{4a(4b)}$	$ENU_{5a(5b)}$ or $ENU_{6a(5b)}$	
LF	w_{lf}	0.5	0.5	0.5		0.5	0.5	
	τ_{lf}	1	1	1		1	1	
FF	w_{ff}	0.5	0.25	$1^{(+)}$	$12^{(-)}$	$1.2^{(+)}$	$3^{(+)}$	$12^{(-)}$
	τ_{ff}	10	15	$10^{(+)}$	$40^{(-)}$	$10^{(+)}$	$10^{(+)}$	$40^{(-)}$

Table 3.8. Parameters used for simulation (Fig. 3.36) of E-DN shown in Figure 3.33. The parameters for soma remain same as in table 3.1.

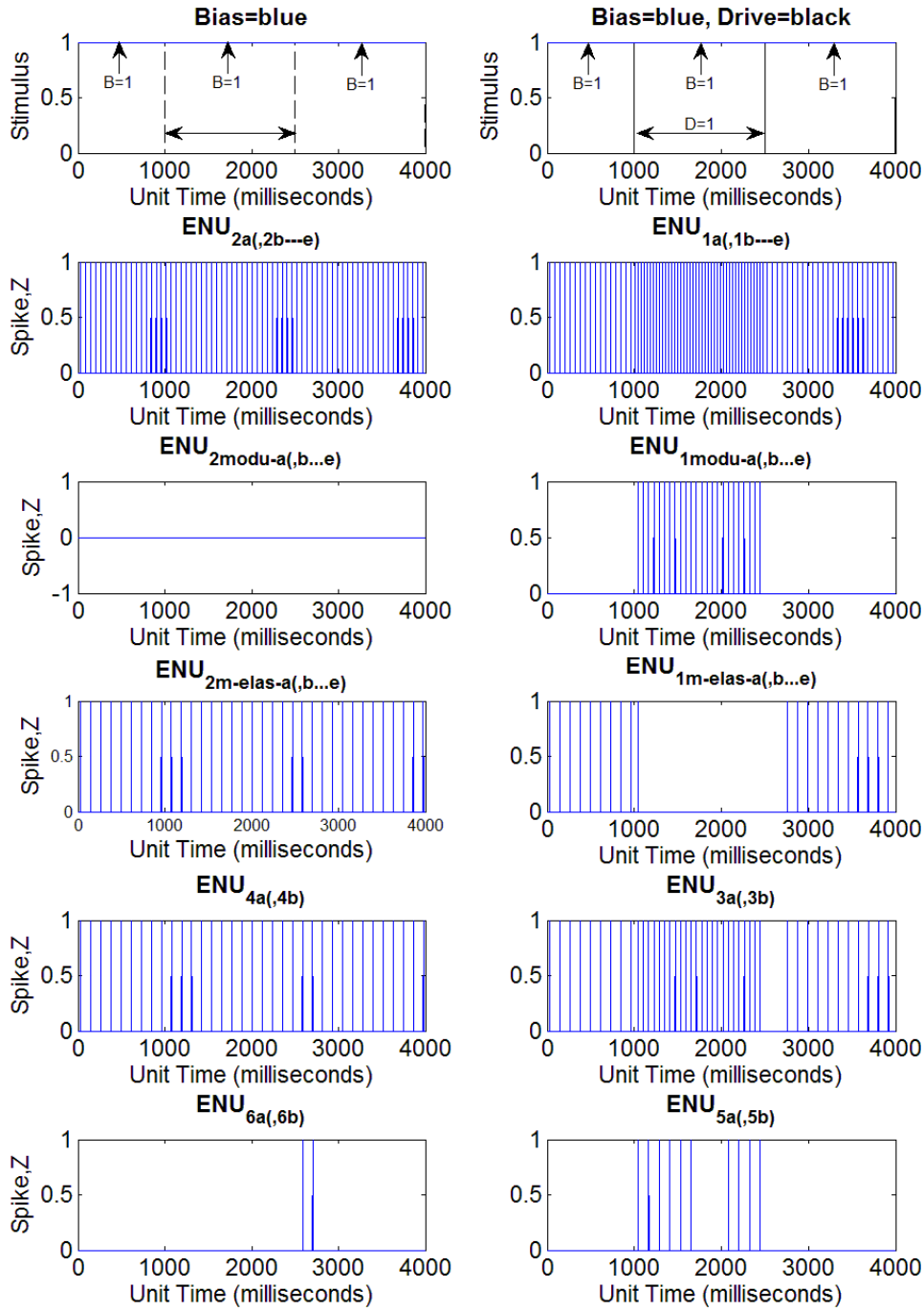

Figure 3.36. Output traces of one basic ENU (ENU_{xa}) implemented (out of 5 each in ENU_1 & ENU_2, 5 each in ENU_{1modu} & ENU_{2modu}, 5 each in $ENU_{1m\text{-}elas}$ & $ENU_{2m\text{-}elas}$, 2 each in ENU_3 & ENU_4 and 2 each in ENU_5 & ENU_6 group) in E-DN architecture of Figure 3.34 & 3.35 receiving both B and D-stimulus using parameters (table 3.8).

Simulation result (Fig. 3.36) for the E-DN (Fig. 3.34 & 3.35) shows that the network has the properties that replicate G-DN seen earlier (Fig. 3.1 & 3.2) and also the elastic property (Fig. 3.6 & 3.7). It should be noted that unlike the earlier output trace (Figure 3.31) the spiking from sixth node after dual-stimuli, though just two spikes, can be considered as an elastic property. This is because the approach that would be implemented for transforming outputs from E-DN to compare the performance of G-DN is based on moving point average.

Pulsed inputs and addition of M-node for the final design (E-N)

As mentioned earlier it should be pointed out that all the designed E-DN's receive DC (constant) input stimulus. Hence for E-DN to be considered a proper PCNN (pulse-coded neural network), the E-DN should be receiving pulsed inputs. That is, basic ENU's of ENU_1 (& ENU_2) and ENU_{1mod} (& ENU_{2mod}) groups within the first two nodes (Eck1 & Eck2) of the E-DN (Fig. 3.35 & 3.36) should receive pulsed inputs corresponding to the DC stimuli. And similarly sensory pulses for the E-N.

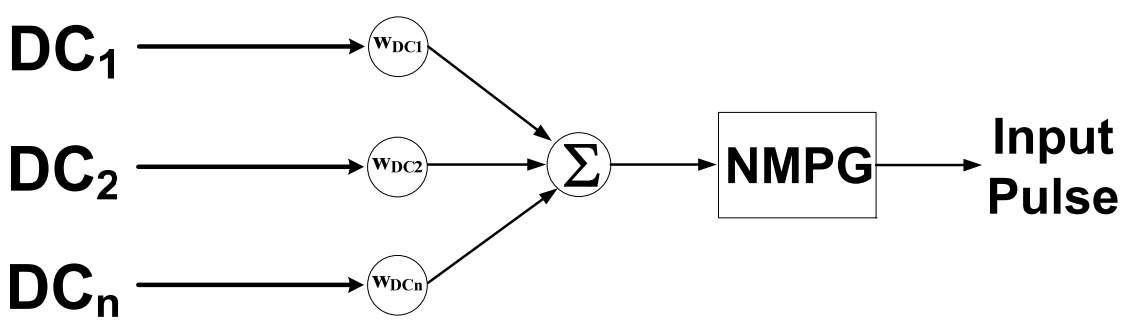

Figure 3.37. General scheme for generating pulsed inputs for E-N architecture shown in Figure 3.38. DC_n is the DC (constant) input for the nth stimulus and w_{DCn} is the weight parameter for respect DC input. Input for the pulse generator (NMPG, neuromime) is therefore $\sum_{\forall n} DC_n \bullet w_{DC_n}$.

Generation of pulsed inputs can be achieved by considering just the neuromime (NMPG) or soma component of the basic ENU such that it receives inputs as the sum of products of DC inputs with respective parameter values (weights), as shown in Figure 3.37. Parameter values of input pulse generators for ENU groups within Eck1 and Eck2, i.e., for ENU_1 (& ENU_2) and ENU_{1mod} (& ENU_{2mod}), and also for the sensory pulses, are shown in table 3.9.

Pulsed Inputs for:	**weights**	**NMPG**		
		V_{pg}	θ_o	τ_{pg}
ENU_1 or ENU_2	$w_B = 0.5$ $w_D = 5 \cdot 10^{-3}$	5	0.5	5
ENU_{1mod} or ENU_{2mod}	$w_B = 5 \cdot 10^{-3}$ $w_D = 0.5$	5	0.5	15
Sensory Pulse	$w_S = 5$	50	0.5	15

Table 3.9. Parameters for pulse generator scheme (Fig. 3.37) for generating input pulses (Fig. 3.38 & 3.39) of E-N architecture shown in Figure 3.39.

Using pulsed inputs in the working architecture of E-DN, the final step is to build the E-N system, i.e., the Eckhorn network (E-N) analogue of Grossberg's network (G-N), which is a dipole network that receives the additional sensory stimulus and whose outputs are sent to a motor node (M-node). Figure 3.38 shows the simulation results (with parameters in table 3.10) during pre-learning stage of the E-N which functionally corresponds to G-N (Fig. 2.7). E-N shown in Figure 3.39 will therefore be the network for comparing the performance with those of G-N to achieve the goal of adaptive PCNN.

ENU Part		E-DN Node							M-Node	
		1 or 2				3 or 4	5 or 6		M	
		ENU Group								
		ENU_1 or ENU_2	ENU_{1modu} or ENU_{2modu}	$ENU_{1m\text{-}elas}$ or $ENU_{2m\text{-}elas}$		ENU_3 or ENU_4	ENU_5 or ENU_6		ENU_M	
		Basic ENU								
		$ENU_{1a(b,\ldots,e)}$ or $ENU_{2a(b,\ldots,e)}$	$ENU_{1modu\text{-}a(b,\ldots,e)}$ or $ENU_{2modu\text{-}a(b,\ldots,e)}$	$ENU_{1m\text{-}elas\text{-}a(b,\ldots,e)}$ or $ENU_{2m\text{-}elas\text{-}a(b,\ldots,e)}$		$ENU_{3a(3b)}$ or $ENU_{4a(4b)}$	$ENU_{5a(5b)}$ or $ENU_{6a(5b)}$		ENU_{Ma}	
LF	w_{lf}	0.5	0.5	0.5		0.5	0.5		0.5	
	τ_{lf}	1	1	1		1	1		1	
FF	w_{ff}	5	5	$1^{(+)}$	$0.5^{(-)}$	$1.2^{(+)}$	$2.5^{(+)}$	$5\bullet10^{-6(-)}$	$2.5^{(+)}$ $5\bullet10^{-6\,(+)}$	$2.5^{(-)}$
	τ_{ff}	10	10	$10^{(+)}$	$30^{(-)}$	$10^{(+)}$	$10^{(+)}$	$30^{(-)}$	$10^{(+)}$	$30^{(-)}$
SOMA	V_{pg}	50	50	50		50	50		50	
	θ_o	0.5	0.5	0.5		0.5	0.5		0.5	
	τ_{pg}	5	5	7.5		7.5	7.5		7.5	

Table 3.10. Parameters for simulation of E-N (Figs. 3.38 & 3.39). ENU_{Ma} FF weights (w_{ff}) = $2.5^{(+)}$ & $2.5^{(-)}$ with E-DN outputs.

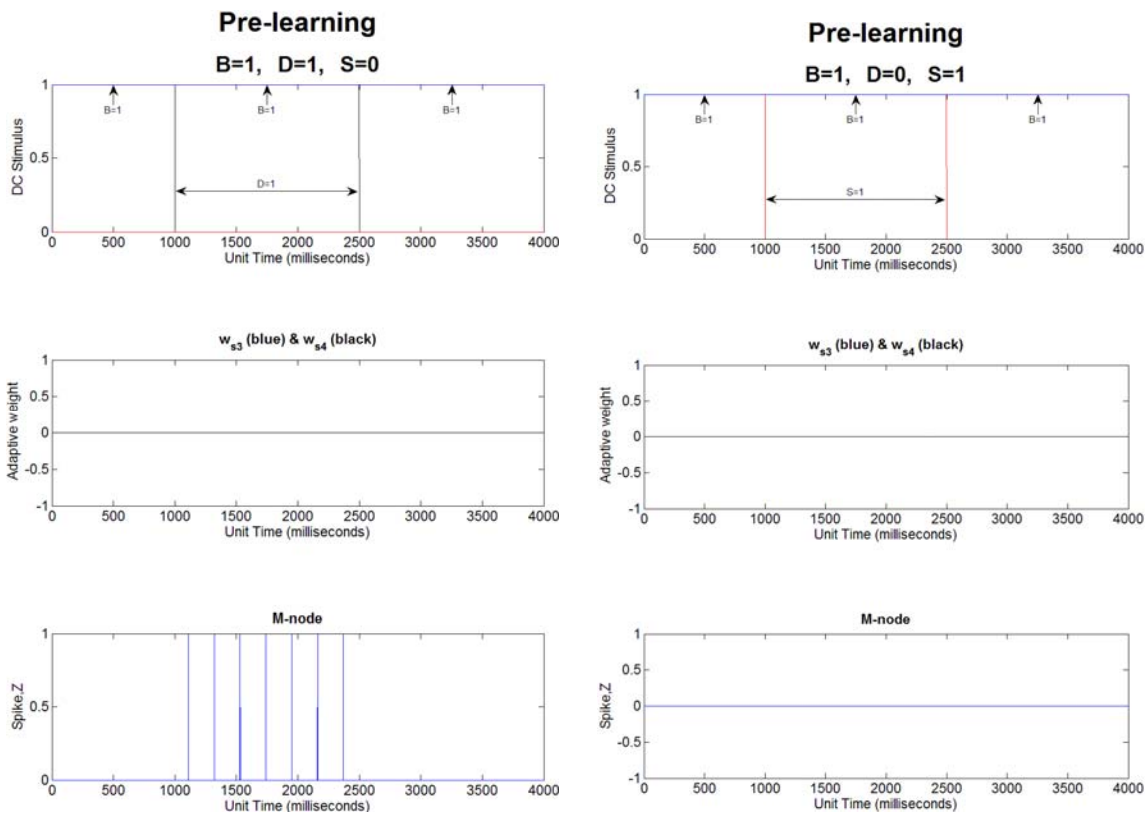

Figure 3.38. Simulation (time-step, Δt=1) of E-N shows network behavior prior to learning/conditioning which corresponds to simulation for G-N seen in Figure 2.7. [plots for pulsed inputs are not shown in this view]

Left: M-node activity (bottom) during B & D stimulus (top) representing unconditioned response to D-stimulus. No learning takes place (middle).

Right: prior to conditioning and hence before association process between conditioning (S) stimulus and unconditioned (D) stimulus, there is no M-node activity (bottom) with S-stimulus.

In both cases w_{s3} and w_{s4} remains zero, i.e., no learning takes place and hence blue (w_{s3}) and black (w_{s4}) values are overlapping.

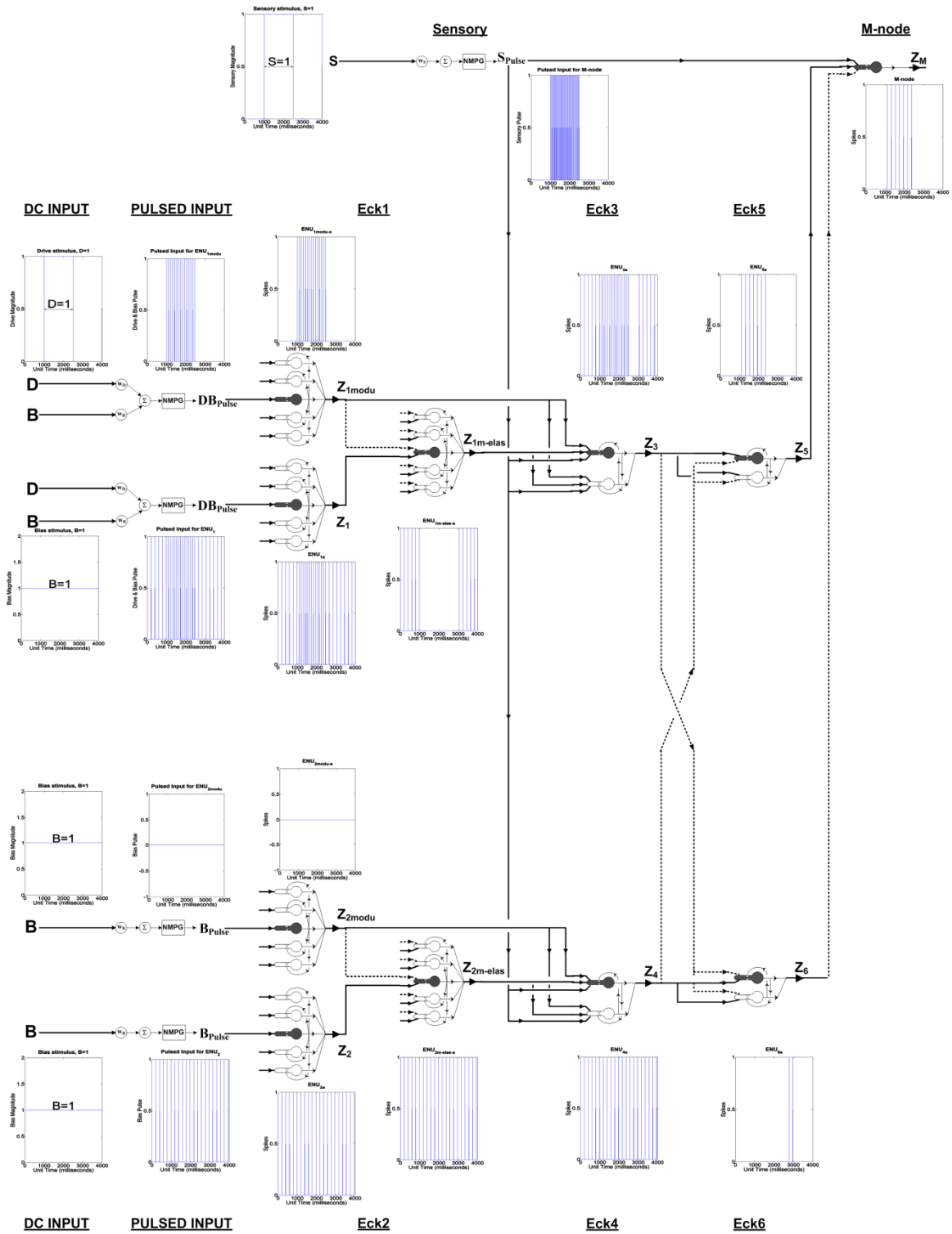

Figure 3.39. E-N for deriving the adaptive PCNN. This E-N is the E-DN (Fig. 3.34 & 3.35) but with input pulses of B, D and also S (sensory) stimulus (Fig. 3.37). The outputs of E-DN, in addition to Sensory pulse (S_{pulse}), are the ENU inputs in M-node (motor node). Notation for the lines representing connection are same as before (solid for excitatory and dashed for inhibitory). The parameters are given in table 3.10.